# QUANTITATIVE ANALYSIS
OF THE
# UREA SYNTHESIS
BY MEANS OF
# LASER RAMAN SPECTROMETRY

MARTIN VAN ECK

# QUANTITATIVE ANALYSIS OF THE UREA SYNTHESIS BY MEANS OF LASER RAMAN SPECTROMETRY

PROEFSCHRIFT

ter verkrijging van de graad van doctor
in de technische wetenschappen
aan de Technische Hogeschool Delft,
op gezag van de Rector Magnificus, prof. dr. J.M. Dirken,
in het openbaar te verdedigen ten overstaan van
het College van Dekanen
op dinsdag 28 mei 1985 te 16.00 uur door

**Martinus van Eck**

scheikundig ingenieur,
geboren te Eindhoven.

Delft 1985

Druk: Dissertatiedrukkerij Wibro, Helmond.

Dit proefschrift is goedgekeurd door de promotor
Prof.dr. L. de Galan

VOORWOORD

Dit proefschrift was nooit tot stand gekomen zonder de hulp van een groot aantal personen binnen en buiten de T.H. Delft. Ik wil allen hiervoor op deze plaats hartelijk danken, maar wil toch ook enkelen met name noemen.

Misschien wat afgezaagd, maar toch wil ik in de eerste plaats mijn promotor, professor Leo de Galan, bedanken. Natuurlijk voor zijn bijdragen tijdens het onderzoek, en vooral ook voor zijn nimmer aflatende ijver mij aan te sporen tot het schrijven van dit proefschrift.

D.S.M. Geleen dank ik voor het betalen van mijn salaris tijdens de laatste periode van het onderzoek en voor de vele vruchtbare discussies die ik mocht voeren met de heren Logemann, de Cooker, de Haan en v.d. Velde.

Nog steeds vind ik het knap hoe Rob Regouw in staat bleek van een kladblaadje een opstelling te maken waarvan ik zelf niet eens wist hoe het eruit moest gaan zien. De vakgroepen Chemische Technologie en Anorganisch Fysisch dank ik voor het beschikbaar stellen van de daarvoor benodigde apparatuur. Van de laatstgenoemde vakgroep wil ik met name Wim Poot danken voor het maken van de vele vullingen voor de hogedruk cel.

Dat voor sommige mensen geldt " haastige spoed is best goed " moge blijken uit de kwaliteit van het teken- en fotowerk, dat vaak op het laatste moment moest worden uitgevoerd. Hiervoor dank ik de heren Frans Bolman, Arie Schriel, C. Warnaar en Fred Hammers.

De goede contacten met een aantal mensen uit het Gebouw voor Analytische Scheikunde hebben er zeker toe bijgedragen dat mijn geplande aanwezigheid van vier jaar uitliep tot bijna zes jaar.

Tot slot dank ik mijn moeder voor alles en natuurlijk Truja, de laatste niet alleen vanwege het vele typewerk.

CONTENTS




Reprinted from
[1]The Analyst, 1983, 108, 485
[2]The Analyst, 1985, 110, 141

# Chapter I GENERAL INTRODUCTION

## 1. Principle

When radiation passes through a transparent material some of it will always be scattered, partially elastically and partially inelastically. In the elastic scattering process the direction of propagation of the incident beam will be changed, not its frequency. If this elastic scattering is caused by the molecules of the medium it is called Rayleigh scattering, after Lord Rayleigh[1] who explained this effect in terms of the classical radiation theory in 1871. If it is caused by particles much larger than the wavelength of the incident radiation, it is called Mie[2] scattering. Hence, if the incident radiation consists of light, Mie scattering can be due to dust particles in the medium.

In the inelastic scattering process the frequency as well as the direction of propagation of the incident beam are changed. In the spectrum of the scattered radiation new pairs of wavenumbers of the type $\nu_o \pm \nu_m$ will be found, where $\nu_o$ is the frequency of the incident radiation and $\nu_m$ is a characteristic frequency belonging to the molecules of the scattering medium. Spectral analysis shows that the frequency $\nu_m$ can be associated with a transition between rotational, vibrational or electronic levels in the scattering system. This effect was predicted on theoretical grounds by Smekal[3] in 1923, and is called the Raman effect, after C.V. Raman[4], who together with K.S. Krishnan, first observed it in 1928.

Raman scattering originates from the interaction between radiation and molecules. The energy level diagrams for the Raman and Rayleigh scattering process are shown in Fig.1. $E_0$ and $E_1$ are energy levels (vibrational, rotational or electronic) of the scattering system, belonging to the ground state and to an excited state, respectively. The level $E_v$ is a virtual level, of which the position depends only on the energy $h\nu_o$ of the incident radiation and on the energy of the level originally occupied by the molecule involved in the interaction. Normally, $E_v$ is not an eigen state of the scattering system. The energy difference $h\nu_m = E_1 - E_0$, which is small compared to the energy $h\nu_o$ of the incident radiation is typical for the molecules involved in the interaction and can be measured in two ways, as can been seen from Fig.1.

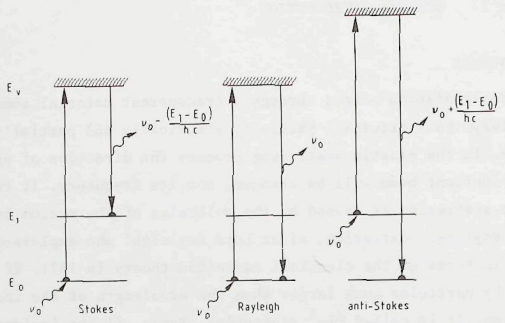


*Fig.1. The energy level diagrams for the Raman and Rayleigh scattering process.*

As the Raman effect is very weak (approximately one Raman photon is produced from a million of incident photons), an intense monochromatic light source is required. Adequate straylight rejection, necessary because of the very intense Rayleigh- and Mie scattering, is only possible with a double monochromator, which makes the technique relatively expensive.

Although in many cases the same transitions in the molecules can be studied with infrared spectroscopy, the methods are, for fundamental reasons, complementary. The enormous upsurge of interest for the Raman effect shortly after its discovery, however, is not surprising, since important structural information could be obtained in spectral regions not yet accessible to infrared spectroscopy. The weakness of the effect, the lack of intense, monochromatic light sources and the development of the competitive infrared absorption instruments, shortly after World War II, caused a decline of this new type of spectroscopy.

Its revival in the early sixties was brought about by the invention of the first laser, the ruby laser, by Maiman[5] in 1960, and nowadays the Raman spectrometer would be inconceivable without a laser (Fig.3). This very intense, monochromatic light source not only offers the possibility to record conventional Raman spectra in a much shorter



time and at much lower sample concentrations, but also enables the recording of Resonance Raman spectra of many compounds and led to the discovery of the non-linear Raman effects. Fig.2 shows the Raman spectrum of $CCl_4$.

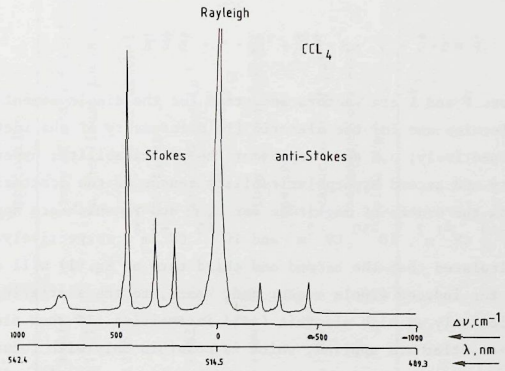


*Fig.2. The Stokes and anti-Stokes Raman spectrum of carbon tetrachloride, recorded with 514.5 nm incident radiation.*

The Resonance Raman effect, a linear Raman effect, occurs when the frequency of the exciting radiation is close to an absorption frequency of the scattering system. As a consequence, the energy level $E_v$, shown in Fig.1 is no longer virtual, but becomes a discrete level. The transition probability is enhanced and resonance takes place, whereby an enormous increase of the intensity of the scattered radiation is achieved. The Resonance Raman effect had been observed for the first time by Shorygin[6] in 1947, but its application became easier thanks to the development of laser systems with a continuously variable frequency, which enable the tuning to the absorption frequency; the experimental set-up is shown in Fig.3.

Contrary to the linear Raman effects, the observation of the non-linear Raman effects would never have been possible without the invention of the laser, since irradiances are required ten orders of magnitude greater than the irradiance produced by solar radiation at the earth's surface. This can be explained as follows. The inten-

sity of the scattered radiation is proportional to the electric dipole induced in the scattering molecules, by the incident radiation. The induced dipole moment itself, however, is a function of the polarizability of the scattering system and of the electric field vector of the incident radiation and can, for the majority of systems, be given by

$$\vec{P} = \alpha \cdot \vec{E} + {}^1/_2 \cdot \beta \cdot \vec{E}\,\vec{E} + {}^1/_6 \cdot \gamma \cdot \vec{E}\,\vec{E}\,\vec{E} \qquad (1)$$

where $\vec{P}$ and $\vec{E}$ are vectors and stand for the dipole moment induced in the molecules and for the electric field intensity of the incident radiation, respectively; $\alpha$, $\beta$ and $\gamma$ represent the polarizability, hyperpolarizability and second hyperpolarizability tensor of the scattering system. From the orders of magnitude for $\alpha$, $\beta$ and $\gamma$, which are approximately $10^{-40}$ $CV^{-1}m^2$, $10^{-50}$ $CV^{-2}m^3$ and $10^{-60}$ $CV^{-3}m^4$, respectively, it can be calculated that the second and third term of Eq.(1) will contribute to the induced dipole moment and, hence, to the scattering of radiation only at high electric field intensities. If such electric field intensities are applied, which is possible only with focussed giant-pulse lasers, the intensity of the scattered radiation will no longer be directly proportional to the intensity of the incident electric field, which explains the term non-linear Raman effects.

In Table 1 the most important non-linear Raman effects are listed. The most promising of these new techniques is certainly Coherent Anti-Stokes Raman Spectroscopy (CARS). To observe the CARS effect two laser beams are required, of different frequencies $\nu_1$ and $\nu_2$ which coincide in the sample. If $\nu_1 - \nu_2$ equals a vibrational frequency of the scattering system, the CARS effect will be observed at the anti-Stokes frequency $\nu_3 = 2\nu_1 - \nu_2$. Hence, the CARS spectrum is obtained by keeping $\nu_1$ fixed and changing the frequency $\nu_2$ (Fig.3).

CARS offers large advantages over conventional Raman spectroscopy. While the spontaneous Raman effect yields only one "Raman photon" for every million incident photons, the CARS method yields at least one "anti-Stokes photon" for every hundred incident photons, which means an improvement of the conversion efficiency by four orders of magnitude. While spontaneous Raman scattering is scattered over the full solid angle of 4 $\pi$ sr, the anti-Stokes scattering at $\nu_3$ in a CARS experiment forms a beam with laser-like properties, which provides a very high light collection by the detector. Since only three



| Effect | First observed by | Application |
|---|---|---|
| Hyper Raman Scattering | P.A. Franken et.al. 1961 [7]<br>W. Kaiser et.al. 1961 [8] | Study of modes forbidden in the linear Raman Effect |
| Stimulated Raman Scatt. | E.J. Woodburg et.al.1962 [9] | Study of vibrational lifetimes |
| Coherent anti-Stokes Raman Scattering (CARS) | R.W. Terhune 1963 [10] | Very low sample concentrations |
| Inverse Raman Scattering | W.J. Jones et.al. 1964 [11] | Study of short-lived species |
| Photoacoustic Raman Scatt. | J.J. Barrett. et.al.1978 [12] | Measurement of gas concentrations even below 1 ppb |

*Table 1. Non-linear Raman Effects.*

frequencies are found in the scattered radiation, no expensive monochromators are required, but filters can be used to separate $\nu_1$ and $\nu_2$ from $\nu_3$. The CARS technique is, however, still difficult to carry out in condensed phases and, hence, is not employed as much as would be expected.

## 2. Analytical use

Since its discovery Raman spectroscopy has been mainly used for qualitative analysis. It has proved to be a valuable technique for fingerprinting and structure analysis. By contrast, quantitative analysis by means of Raman spectroscopy has suffered from the low sensitivity of the spontaneous Raman effect. Low detection limits were only found in the limited cases where Resonance Raman or Surface Enhancement[13] techniques could be applied, and for very strong scatterers. As a consequence, Raman spectroscopy is not a technique which is frequently applied for quantitative analysis. Nevertheless it offers a number of advantages with respect to other, spectroscopic and non-spectroscopic, quantitative analysis techniques.

Raman spectroscopy is a non-destructive technique, like infrared- and ultraviolet absorption spectroscopy. Since visible radiation, i.e. light, can be and, in most cases, will be used to record Raman spectra, optical components which transmit in the visible region of the spectrum can be used. Hence, lenses, cells etc. made of ordinary glass are applied. As water is a poor scatterer, it is an excellent solvent for Raman spectroscopy. Relatively strong water bands are only observed in the spectral region where O-H and N-H vibrations are found and, hence, they hardly interfere with the Raman bands of most other compounds.

## 3. The present study

In this study we will demonstrate that the spontaneous Raman effect can be used for in-situ quantitative analysis at conditions of elevated temperature and pressure. As an example we have chosen the synthesis of urea. Urea is formed in a two-step reaction:

$$2NH_3 + CO_2 \rightleftarrows H_2NCOONH_4 \qquad (2)$$

$$H_2NCOONH_4 \rightleftarrows H_2NCONH_2 + H_2O \qquad (3)$$



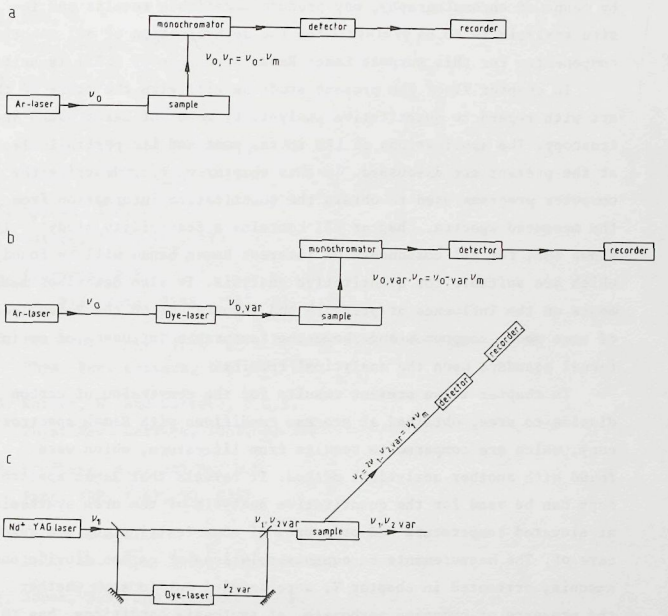


*Fig.3. The set-up for the observation of (a) the spontaneous Raman effect, (b) the Resonance Raman effect and (c) the Coherent anti-Stokes Raman effect (CARS).*

Normal synthesis conditions are a temperature range from 170° to 210° C and a pressure range from 15 to 25 MPa[14]. A change of pressure or temperature will give a considerable change in the composition of the reaction mixture. Hence, sampling and off-line analysis, for example by means of chromatography, may produce unreliable results and in-situ analysis is to be preferred for the determination of all reaction components. For this purpose Laser Raman spectroscopy (LRS) is suitable.

In chapter II of the present study we will give the state of the art with regard to quantitative analysis by means of Laser Raman spectroscopy. The applications of LRS in the past and its possibilities at the present are discussed. In this chapter we also describe the computer programs used to obtain the quantitative information from the measured spectra. Chapter III contains a feasibility study[15]. It shows that for all components of interest Raman bands will be found, which are suitable for quantitative analysis. It also describes measurements on the influence of pressure and temperature on the Raman spectra of some model compounds and shows the favourable influence of an internal standard upon the analytical results.

In chapter IV we present results for the conversion of carbon dioxide to urea, obtained at process conditions with Raman spectroscopy, which are compared to results from literature, which were found with another analytical method. It reveals that Raman spectroscopy can be used for the quantitative analysis of the urea synthesis at elevated temperature and pressure, if some restrictions are taken care of. The measurements on aqueous solutions of carbon dioxide and ammonia, presented in chapter V, were carried out to show whether the presence of hydrogen carbonate, at synthesis conditions, has to be expected, or not. Possibly the bicarbonate ion is an intermediate in the urea formation. This chapter also demonstrates that low sensitivity is not necessarily the only restraint for this spectroscopic technique and shows the limitations of the method presented in this study.



*REFERENCES*


1. Lord Rayleigh,
   Phil. Mag., 1871, XLI, 274, 447
2. Mie, G.
   Ann. Physik, 1908, 25, 377
3. Smekal, A.
   Naturwiss., 1923, 11, 873
4. Raman, C.V. and Krishnan, K.S.
   Nature, 1928, 121, 501
5. Maiman, T.H.
   Nature, 1960, 187, 493
6. Shorygin, P.P.
   Zh. Fiz. Khim. SSSR, 1947, 21, 1125
7. Franken, P.A., Hill, A.E., Peters, C.W. and Weinreich, G.
   Phys. Rev. Letters, 1961, 7, 118
8. Kaiser, W. and Garrett, C.G.B.
   Phys. Rev. Letters, 1961, 7, 229
9. Woodburg, E.J. and Ng, W.K.
   Proc. IRE, 1962, 50, 2367
10. Terhune, R.W.
    Bull. Am. Phys. Soc., 1963, 8, 359
11. Jones, W.J. and Stoicheff, B.P.
    Phys. Rev. Letters, 1964, 13, 657
12. Barrett, J.J. and Berry, M.J.
    "Photoacoustic Raman Scattering in Gases",
    Proc. of the 6th Conf. on Raman Spectrosc., Bangalore, India 1978
    Schmid, E., Krishnan, R., Kiefer, W., and Schrotter, H.
    Eds. Heyden, London, 1978, Vol. 1, 466
13. Van Duyne, R.F.
    "Chemical and Biological Applications of Lasers",
    Moore, C.B., ed., Vol. 4, Academic Press, New York, 1979

14. Lemkowitz, S.M.
"Phase and Corrosion Studies of the Ammonia-Carbon Dioxide-Water System at the Conditions of the Hot Gas Recirculation Process for the Synthesis of Urea", Thesis, Delft, 1975

15. Van Eck, M., Van Dalen, J.P.J. and De Galan, L.
Analyst, 1983, 108, 485



## Chapter II QUANTITATIVE ANALYSIS

### 1. Introduction

Since its discovery, about sixty years ago, Raman spectrometry has grown from a cumbersome, time consuming technique to an easily applicable, relatively fast spectroscopic method, as far as qualitative analysis is concerned. Quantitative analysis by means of Raman spectrometry, however, has never been able to keep up with this development, as can been seen from the small number of articles on quantitative analysis: about half a percent of all articles on the subject over the last decade. This is caused partly by the low sensitivity of the method, which makes it difficult to study dilute solutions, adsorbed species, gases, etc., but also by the fact that a measured Raman intensity cannot be translated straightforward into a concentration. As a result, Raman spectrometry was used only in those cases where other spectroscopic methods failed. One particular example is the determination of ionic species in aqueous solution, which is indeed a favorite subject of quantitative analysis by means of Raman spectrometry.

Interactions between cations, anions and water have been extensively studied by many investigators. Information was obtained with respect to ion-pair formation, residence times etc., on various aqueous solutions of metal/nitrate[1-6] and metal/nitrite[7,8] systems; other solvents like deuterium oxide[9] and acetonitrile[10] have also been used. The method proved to be reliable for the study of the ionization of acids[11-15] and of kinetics of the catalyzed hydrolysis of acetonitrile[16]. Detection limits were determined for several solutes in aqueous solutions[17-19].

Apart from articles on species in solution, publications have appeared that show the applicability of Raman spectrometry for quantitative analysis of solid samples. The technique was used for example to determine phase ratios[20] and concentrations of impurities[21] and for the characterization of polymers[22-26].

With the improvement of light sources, dispersing systems and detectors, analysis of gaseous samples also became easier. In addition to measurements on natural gas mixtures[27,28] and mixtures of hydrogen-isotopes[29-31], measurements were performed to determine gas concentrations in turbulent diffusion flames[32].

In this chapter we intend to show what information is needed to derive concentrations from Raman intensities. For samples with an unknown composition quantitative analysis must always be preceeded by qualitative analysis. If the composition of the sample is known, however, or if we are interested only in species known to be present in the sample, this is not necessary and we can directly record the spectral regions of interest. It is a prerequisite of course that the Raman spectra of the pure species are known, to be able to select the bands we use for quantitative analysis.

In general the intensity of a Raman band measured as the height or the integrated area, will be directly proportional to the concentration of the compound. As the intensity is influenced not only by the concentration, but also by many other factors, it is generally not possible to derive the concentration directly from the absolute intensity of the scattered radiation. Factors affecting the intensity of the scattered radiation apart from the concentration, are

- the intensity of the incident radiation
- the frequency of the incident radiation
- the index of refraction of the sample
- the colour of the sample
- sample positioning and cell windows
- instrumental parameters

For the linear Raman effect, the relationship for the intensity of the radiation scattered by a species A can be given by

$$I_{r,A} = I_o \cdot [A] \cdot I_{m,A} \cdot (F_1 \cdot F_2 \ldots F_n) \qquad (1)$$

where $I_{r,A}$ is the measured Raman intensity, $I_o$ is the intensity of the incident radiation, [A] is the concentration of the species, $I_{m,A}$ is the molar Raman intensity of the species and $F_1 \ldots F_n$ are fundamental and instrumental parameters. Some of these parameters can be controlled, others have to be corrected for. It will be shown in this chapter that the internal standard plays an important role in quantitative Raman spectrometry.

In general, the low sensitivity of the Raman effect is a disadvantage if quantitative analysis is concerned. Therefore, detection limits must be determined and it must be shown that the concentration of all compounds to be measured exceeds the detection limit.



Another problem may arise from the fact that every compound has a Raman spectrum, composed of one or more bands. Hence, if the spectrum of a mixture is recorded severe band overlap may occur, which complicates the determination of the band intensities and thus the calculation of the concentrations. To overcome the problems due to band overlap computer programs are used to calculate the contributions of the individual bands in the band envelope.

## 2. The influence of instrumental factors on Raman intensities

### 2.1. Introduction

The equipment necessary for the observation of Raman spectra consists of four essential components, namely a source of monochromatic radiation, a dispersing system, a detection system and a sample cell. Each of these components will affect the measured Raman intensities. As will be shown, however, the influence of the first three can be controlled and corrected for. The discussion on the influence of the sample cell is postponed to II-4.

### 2.2. The source of monochromatic radiation

The contemporary Raman spectrometer uses a laser, because it is the source of choice for intense, monochromatic radiation. With an argon-ion laser used in this study, two powerful lines, at wavelengths 488.0 nm and 514.5 nm, are available, together with some weaker lines. Tuning to one line can be achieved by means of a prism, placed inside the laser cavity. The intensity of the radiation can be adjusted continuously from zero to maximum power, which, in our case, is approximately 1 Watt for the 514.5 nm line and 0.8 Watt for the 488.0 nm line. The typical band width of a line produced by a laser operating in the multimode is approximately 0.2 $cm^{-1}$. By placing an etalon inside the laser cavity single-mode operation is obtained and the band width is reduced to approximately 0.001 $cm^{-1}$, which induces 50 per cent power loss. Single-mode operation is useful only for the determination of the rotational fine-structure in gas phase samples, where high resolution is mandatory. In the Raman spectrometry of liquids rotational fine-structure is lost and multi-mode operation is satisfactory.

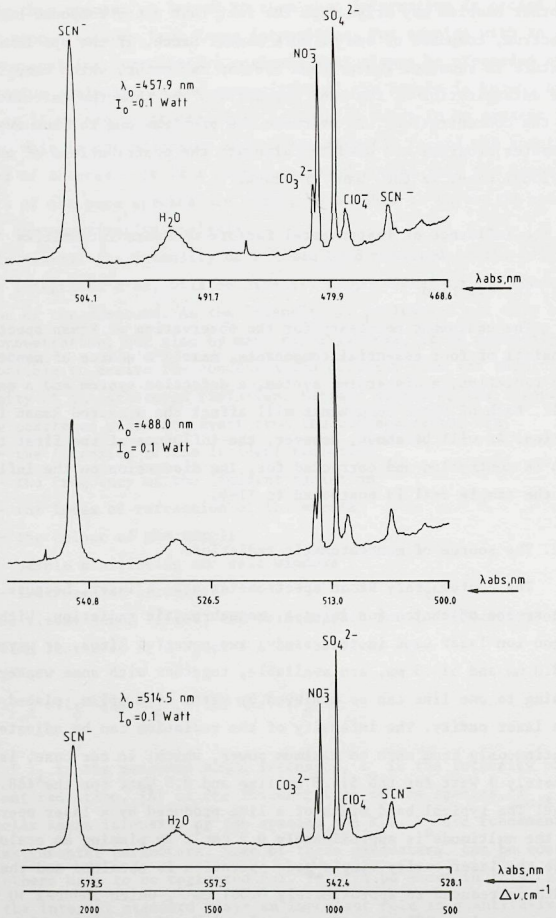


*Fig.1. The Raman spectra of an aqueous solution of potassium salts, recorded with different incident wavelengths.*



A built-in feed-back system provides a stable power output. Short-term power fluctuations are less than 1%. As the intensity of all Raman bands is directly proportional to the intensity of the incident radiation, day-to-day power changes are compensated for by the use of an internal standard.

Visible radiation is usually preferred for Raman spectrometry, because the laser lines are strongest in that region and disturbance by sample fluorescence is less. The wavelength range of a Raman spectrum varies with the incident wavelength. However, the characteristic feature of the Raman transition is its frequency shift from the incident line. (cf. Fig.1). In addition, the intensity of a Raman band is proportional to the fourth power of its frequency[33]. The intensity ratio of a band observed with two different incident lines is given as

$$\frac{I(\nu)}{I(\nu')} = \frac{I(\nu_0-\nu_m)}{I(\nu_0'-\nu_m)} = \left[\frac{\nu_0-\nu_m}{\nu_0'-\nu_m}\right]^4 \qquad (2)$$

where I is the intensity of the Raman band with frequency shift $\nu_m$ and $\nu_0$ and $\nu_0'$ are frequencies of the incident radiation. From this equation it is obvious that the ratio $I(\nu)/I(\nu')$ is a function of $\nu_0$ and $\nu_m$. Hence, if spectra recorded with sources of different frequency, are compared, corrections must be made for this effect. Changing the frequency of the source from 20492 $cm^{-1}$ (488.0 nm) to 19436 $cm^{-1}$ (514.5 nm) results in a decrease of the intensity by 25 and 28% for bands at 1000 and 3000 $cm^{-1}$, respectively. Therefore, the effect is fairly small for the spectra shown in Fig.1. In this study all spectra are recorded using the 514.5 nm line at maximum power. Raman shifts from 50 to 4000 $cm^{-1}$ then cover a wavelength range of 515-650 nm.

## 2.3. The dispersing system

The dispersing system is a vital part of a Raman spectrometer, because all spectral information is obtained in a relatively small range (100 nm) at the high-wavelength side of the Rayleigh band. Therefore factors like resolving power, dispersion and slit width are of

great importance. As Rayleigh scattering, is three orders of magnitude more intense than Raman scattering, a system must be used with high stray-light rejection. For these reasons, in general, a double monochromator is used.

If extreme stray-light rejection is necessary, the use of a triple monochromator should be considered, because the additional monochromator results in a decrease of stray light by approximately five orders of magnitude. Studies which require extreme resolution, i.e. the determination of rotational fine-structures etc., benefit from the use of interferometric techniques.

Our equipment contains a double monochromator of the type Jobin Yvon Ramanor HG-2S. Its specifications are listed in Table 1.

| | |
|---|---|
| Monochromators | Double monochromator equipped with two concave holographic gratings. Focal length: 1000 mm, Aperture: f/8 |
| Spectral range | Mechanical: 32258-11494 $cm^{-1}$ (310-870 nm) Visible version: 22720-12500 $cm^{-1}$ (440-800 nm) |
| Resolution | Better than 0.5 $cm^{-1}$ at 514.5 nm. |
| Diffused light | $10^{-14}$ at 20 $cm^{-1}$ from the exciting line. |
| Slits | Straight, height 20 mm, width adjustable with vernier and stepping motor for each slit (4). |

*Table 1. Specifications of the Jobin Yvon Ramanor HG-2S double monochromator.*

## 2.4. The detection system

In most Raman spectrometers the detection system is composed of a photomultiplier, an amplifier and a recorder. At the extremely low light levels, frequently encountered in Raman spectrometry, the dark current can be reduced by cooling the photomultiplier. The signal from the detector is processed by a d.c-amplifier, a lock-in amplifier or a photon counting device. For very low light levels photon counting or lock-in amplification are to be preferred. For moderate to high levels direct current amplification is cheaper and sufficient.

The sensitivity of a photomultiplier strongly depends on the wavelength of the incident radiation. This is another reason why in



quantitative Raman spectrometry the use of a fixed source wavelength is recommended. Comparing Raman spectra recorded with different incident radiation is only possible when the sensitivity/wavelength characteristics of the photomultiplier are known.

# 3. Influence of sample characteristics on Raman intensities

## 3.1. Introduction

Several sample characteristics may influence absolute and relative Raman intensities. It is found for example that molar Raman intensities depend on the refractive index of the sample. Solvent/solute interactions may also effect Raman intensities, as well as the colour of the sample. It will be shown, however, that the effects mentioned here are of minor importance in the present study.

## 3.2. The index of refraction

Molar Raman intensities increase considerably in passing from the gaseous to the condensed phase. This phenomenon is caused by the action of local field effects in the liquid phase. As the local field effect is a function of the refractive index of the sample, molar Raman intensities may change if the index of refraction of the sample changes e.g. as a result of temperature or concentration change. Eckhardt and Wagner[34] give as the most appropriate correction factor (L) for the local field effect in Raman spectrometry

$$L = \frac{n_s}{n_o} \cdot \frac{(n_s^2 + 2)^2 \, (n_o^2 + 2)^2}{81} \qquad (3)$$

where $n_s$ and $n_o$ are, respectively, the index of refraction at the frequency of the Raman band and at the frequency of the incident radiation Considering that the wavelength range of a Raman spectrum is small and hence, the difference between $n_o$ and $n_s$ is negligible, Eq.(3) can be approximated by

$$L = \left[\frac{n_s^2 + 2}{3}\right]^4 \qquad (4)$$

As $n_s$ is a function of the concentration, a curved calibration line is found for absolute Raman intensities. If an internal standard is used, however, the value of L, Eq.(4) is equal for sample and standard and, hence, the calibration curve should be a straight line.

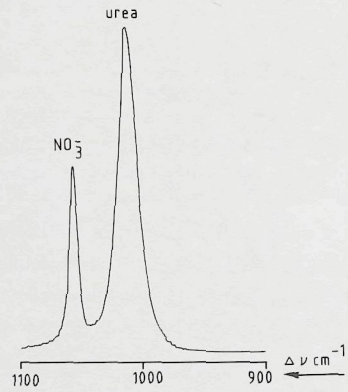


*Fig.2. The Raman spectrum of an aqueous solution of urea ( 1.62 Mol.$l^{-1}$ ) and potassium nitrate.*

To study this effect aqueous solutions of urea were prepared ranging from 0.2 to 3.6 Mol.$l^{-1}$, using potassium nitrate as internal standard. The intensities of the 1005 cm$^{-1}$ band of urea and of the 1050 cm$^{-1}$ band of $NO_3^-$ were determined from the Raman spectra and the refractive indices of the solutions were measured.
Fig.2 shows the Raman spectrum of one of these solutions. The relative intensity of the urea band was defined as

$$I_{urea,\,rel.} = \frac{I_{urea}}{I_{NO_3^-}} \cdot [NO_3^-] \qquad (5)$$



where $I_{urea}$ and $I_{NO_3^-}$ are, respectively the integrated area of the 1005 cm$^{-1}$ band of urea and of the 1050 cm$^{-1}$ band of $NO_3^-$ and $[NO_3^-]$ is the nitrate concentration. Fig.3 shows the relative intensity of the urea band as function of the urea concentration. In this figure the scale for the index of refraction is also added.

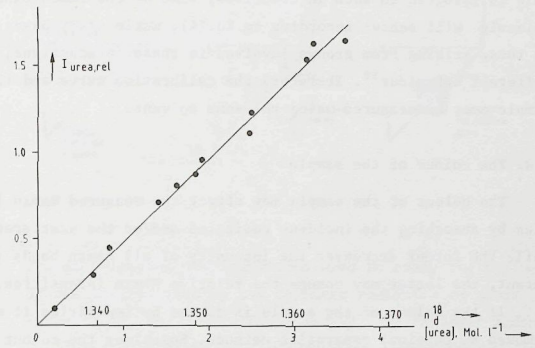


*Fig.3. Calibration curve for aqueous solutions of urea, using potassium nitrate as internal standard. On the concentration axis the scale for the refractive index is also shown.*

It is obvious from Fig.3 that the calibration curve for aqueous solutions of urea is a straight line, if $NO_3^-$ is used as internal standard. The value of the coefficient of determination for the line, which was calculated by means of linear regression, exceeds 0.99. Hence, the use of $NO_3^-$ as internal standard corrects for changes of the local field effect, over the refractive index range from 1.33 to 1.37.

### 3.3. Solvent effects

The equations used above to show the influence of the index of refraction on Raman intentities, can also be used to calculate the effect of different solvents on the Raman intensities of solutes. This effect may be much more pronounced, because of the large difference between the values of the refractive index of several solvents. In most cases

good agreement is found between the experimental results and values derived from Eq.(4); exceptions are also found however[35-38].

As Eq.(4) only corrects for changes of the internal electric field to which the molecules are exposed, the deviations from theoretical behaviour are ascribed to specific intermolecular interactions, such as hydrogen bonding. Since, in general, only a part of the molecule is involved in such interactions, some of the Raman bands of the molecule will behave according to Eq.(4), while other bands, especially those arising from groups involved in these interactions, show a different behaviour[38]. Therefore the calibration curve and the unknown sample must be measured using the same solvent.

### 3.4. The colour of the sample

The colour of the sample may effect the measured Raman intensities by absorbing the incident radiation and/or the scattered radiation. While the former decreases the intensity of all Raman bands to the same extent, the latter may change the relative Raman intensities.

If the colour of the sample is caused by impurities it may be removed by physical separation methods. Sometimes the colour disappears spontaneously as a result of thermal degradation of the impurities by the laser radiation.

If the colour is an intrinsic property of the sample serious changes of the relative Raman intensities may occur. Generally, the intensity of most bands decreases due to absorption of the incident or scattered radiation. If, however, the excitation frequency is close to the absorption band of the sample the intensities of some specific bands may increase by many orders of magnitude as a consequence of the resonance Raman effect[39].

For urea synthesis mixtures no problems are expected, because the components, i.e. urea, carbamate, water, carbon dioxide and ammonia, do not absorb radiation in the visible part of the spectrum.

## 4. Influence of sample positioning and cell windows on Raman intensities

### 4.1. Introduction

Sample positioning and cell windows may severely affect Raman intensities. Obviously, the sample cell should be carefully aligned



and its windows clean. Other effects may arise, however from the polarized nature of the Raman radiation.

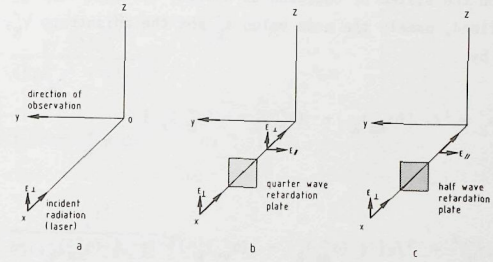


*Fig.4. The experimental configurations used to study the influence of the polarization of the incident radiation on Raman intensities, (a) conventional set-up, (b) incident radiation depolarized by means of a quarter-wave retardation plate and (c) direction of polarization turned over 90° by means of a half-wave retardation plate.*

### 4.2. Polarization

Fig. 4a shows the instrumental configuration used in this study. The laser transmits linearly polarized radiation in the x-direction with the electric vector in the z-direction, while the y-axis is the direction of observation. A scattering molecule is located in the origin of the system.

For Raman scattering the interaction between the molecule and the incident radiation is given by

$$\vec{P} = [\alpha']_k \cdot \vec{E} \qquad (6)$$

where $\vec{P}$ is the induced dipole moment, $\vec{E}$ is the electric vector of the incident radiation and $[\alpha']_k$ is the derived polarizability tensor for the vibration k. Although the values of the matrix components $\alpha'_{ij}$ depend on the system of coordinates chosen, two invariant quantities may be defined, namely the mean value $a'_k$ and the anisotropy $\gamma'_k$, which are given by

$$a'_k = {}^1/_3 \left[(\alpha'_{xx})_k + (\alpha'_{yy})_k + (\alpha'_{zz})_k\right] \tag{7}$$

and

$$(\gamma'_k)^2 = {}^1/_2\left[ \left( (\alpha'_{xx})_k - (\alpha'_{yy})_k \right)^2 + \left( (\alpha'_{xx})_k - (\alpha'_{zz})_k \right)^2 + \left((\alpha'_{yy})_k - (\alpha'_{zz})_k\right)^2 + 6\left((\alpha'_{xx})^2_k + (\alpha'_{yy})^2_k + (\alpha'_{zz})^2_k\right)\right] \tag{8}$$

Both $a'_k$ and $\gamma'_k$ are molecular quantities which depend only on the type of vibration.

The interaction between a vibrating molecule and electromagnetic radiation results in a dipole oscillating with a frequency which is a superposition of the frequency of the normal vibration of the molecule and the frequency of the incident radiation. This oscillating dipole is the source of Raman scattering. The scattering intensity depends on the direction of observation. A maximum value is found in directions perpendicular to the dipole, whereas the intensity is zero in the direction of the dipole.

From Eq.(6) it can be seen that the direction of the induced dipole depends on the state of polarization of the incident radiation and on the symmetry properties of the vibration involved. Hence, the polarization properties of the scattered radiation show the same dependence.

The depolarization ratio $\rho$ of the scattered radiation is defined as $I_{//}/I_{\perp}$, where $I_{//}$ and $I_{\perp}$ are the intensities of the scattered radiation with the electric vector parallel and perpendicular to the xy-plane, respectively. The value of $\rho$ depends on the properties of the incident radiation. It is customary to distinguish $\rho_n$ for natural incident radiation, $\rho_{\perp}$ for linearly polarized incident radiation with



$\vec{E} \perp xy$ and $\rho_{//}$ for linearly polarized incident radiation with $\vec{E} // xy$. For a collection of molecules, randomly oriented in space, it can be derived that:

$$\rho_{\perp} = \frac{3(\gamma'_k)^2}{45(a'_k)^2 + 4(\gamma'_k)^2} \tag{9}$$

$$\rho_{//} = 1, \text{ for } \gamma'_k \neq 0 \tag{10}$$

$$\rho_n = \frac{6(\gamma_k)^2}{45(a'_k)^2 + 7(\gamma'_k)^2} \tag{11}$$

A Raman band is called depolarized if $a'_k = 0$, so that $\rho_{\perp} = {}^3/_4$ or $\rho_n = {}^6/_7$; in that case the equilibrium symmetry of the molecule is not preserved during the vibration. A band is polarized if $a'_k \neq 0$, so that $0 < \rho_{\perp} < {}^3/_4$ or $0 < \rho_n < {}^6/_7$; if $\rho_{\perp}$ or $\rho_n = 0$ it is said to be completely polarized. The depolarization ratio is a good aid for the attribution of unknown bands to molecular vibrations.

From the treatment above it is clear that Raman intensities depend on the intensity as well as on the polarization properties of the incident radiation. The influence of the intensity can always be compensated for by an internal standard. The influence of a change of the polarization, however, can only be compensated by an internal standard if the sample band and the standard band have the same depolarization ratio. This is illustrated by a measurement of the Raman intensity of some carbon tetrachloride bands.

The bands investigated were: the symmetric stretching vibration at 460 $cm^{-1}$ and two bending vibrations at 220 $cm^{-1}$ and 320 $cm^{-1}$, respectively. The sample was contained in a glass cell which does not influence the state of polarization of the incident or scattered radiation. By means of retardation plates three different states of polarization were created for the incident radiation. In Fig.4 the set up for the measurement is shown. In Table 2 the results are given; it shows the intensity ratios $I_{220\ cm^{-1}}/I_{320\ cm^{-1}}$ and $I_{220\ cm^{-1}}/I_{460\ cm^{-1}}$ for the various configurations.

| | $\vec{E}_{\perp}$ | $\vec{E}_{\perp} + \vec{E}_{//}$ | $\vec{E}_{//}$ |
|---|---|---|---|
| $\frac{I_{220\ cm^{-1}}}{I_{320\ cm^{-1}}}$ | 0.92 | 0.91 | 0.91 |
| $\frac{I_{220\ cm^{-1}}}{I_{460\ cm^{-1}}}$ | 0.36 | 0.68 | 7.33 |

*Table 2. Influence of the state of polarization of the incident radiation on the ratio of the Raman intensities of three $CCl_4$ bands.*

Obviously, the intensity ratio of the 220 $cm^{-1}$ and 320 $cm^{-1}$ band is not affected by the state of polarization of the incident radiation, whereas a significant change is found for the ratio $I_{220}/I_{460}$. This result is in good agreement with the depolarization ratios ($\rho_{\perp}$) of these bands which are 0, 0.75 and 0.75 for the 460 $cm^{-1}$, 220 $cm^{-1}$ and 320 $cm^{-1}$ band, respectively.

This measurement shows that, generally, an internal standard does not correct for changes of the state of polarization of the incident radiation. Normally this will have no consequences for quantitative measurements as long as glass cells are used, because glass does not influence the polarization properties of radiation. For the measurements at high pressure, however, glass is unsuitable and sapphire cell windows or sapphire cells are used. As sapphire is a birefringent material, it may change the polarization properties of the incident and the scattered radiation. Therefore, if sapphire is used polarization problems must be prevented by ensuring fixed cell windows and a reproducible sample positioning.

## 5. The determination of band intensities from Raman spectra

### 5.1. Introduction

The intensity of a Raman band can be defined either as the height, or as the integrated area of that band. If the spectrum is composed of free lying bands only, it is easy to determine the band intensities by means of a ruler or a simple integrator. For spectra



of more complex molecules and for spectra of mixtures, problems may arise due to band overlap. In less severe cases a sophisticated, microprocessor operated integrator may still be able to calculate the contribution of the separate bands. If strong overlap occurs computer operated curve-fit programs must be used. An example is the determination of the Raman intensities of urea and carbamate from spectra of urea synthesis mixtures, as can be seen from Fig.5. In the following sections we will describe the programs used to calculate the contributions of the separate bands to the Raman band envelope.

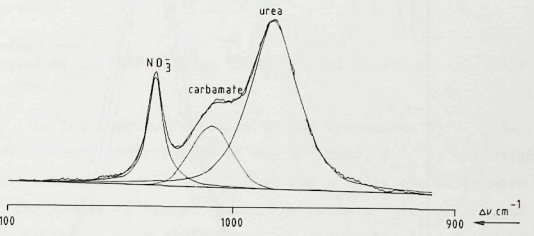


*Fig.5. The Raman spectrum of a urea synthesis mixture at process conditions. The initial molar ratios $NH_3/CO_2$ and $H_2O/CO_2$ were 5.0 and 0.0, respectively, t = 184 °C and p = 30 MPa. Potassium nitrate was used as internal standard.*

### 5.2. The basic curve fit program

Generally, the profile of a Raman band is a Voigt function, which is a convolution of a Lorentzian and Gaussian profile[40]. Therefore, we decided to use the program PC-116 of Pitha and Jones[41].

This program, written in Fortran-IV, was developed to fit infrared absorption spectra. Since combined Gauss-Lorentz functions were used, it could readily be adapted to fit Raman spectra; only some minor changes had to be made with respect to the data input section. The program can fit sets of either Gauss, Lorentz or combined Gauss-Lorentz functions through a measured spectrum. The combined function is the sum or product of two coincident functions of variable inten-

sity. The Gauss/Lorentz width ratio must be chosen in advance and is fixed during the iteration procedure. From a great number of different spectra we determined that the best results are obtained if a Gauss/Lorentz sum function is used, with a value of 1.4 for the ratio $Width_{Gauss}/Width_{Lorentz}$. In Fig.6 the separate Gauss and Lorentz profiles are shown, together with the profile of the combined Gauss/Lorentz sum function.

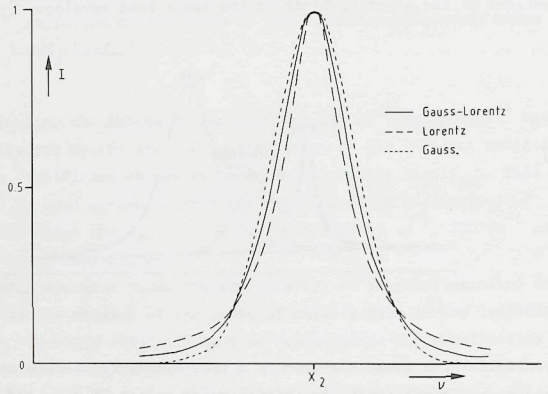


*Fig.6. Separate Gauss and Lorentz profiles and the profile of the Gauss/Lorentz sum function. The ratio $Width_{Gauss}/Width_{Lorentz}$ is 1.4 (i.e. $x_4/x_3=0.6$) and the contributions in height are equal, hence $x_1=x_5$.*

The program starts by calculating a baseline through the measured spectrum. It is calculated as a straight line, using linear regression. Although any part of the spectrum may be chosen for this calculation, normally the first and last 25 datapoints are used. The baseline is subtracted from the measured spectrum.

Then, in an iterative procedure, the band parameters are varied in order to minimize $\Phi$, where



$$\Phi = \sum_{1}^{n} (I_{obs,n} - I_{calc,n})^2 \qquad (12)$$

with n is the number of datapoints, $I_{obs,n}$ is the observed Raman intensity of the $n^{th}$ point and $I_{calc,n}$ is the calculated Raman intensity for the $n^{th}$ point. For the Gauss/Lorentz sum function $I_{calc,n}$ is given by

$$I_{cal,\nu} = \sum_{p=1}^{m} [\, x_{1,p}(1+x_{3,p}^2\,(\nu-x_{2,p})^2\,)^{-1} + x_{5,p} \cdot \exp - (x_{4,p}^2\,(\nu-x_{2,p})^2\,)\,] \qquad (13)$$

where $I_{calc,\nu}$ is the computed ordinate at the wavenumber $\nu$, $x_{1,p}$ is height of the Lorentz contribution of the $p^{th}$ band, $x_{5,p}$ is the height of the Gauss contribution of the $p^{th}$ band and $x_{2,p}$ is the wavenumber position of the center of the $p^{th}$ band. The ratio $x_{4,p}/x_{3,p}$ is equal to the ratio $Width_{Lorentz} \cdot \sqrt{\ln 2}/Width_{Gauss}$ and is fixed at 0.6.M is the number of constituent bands in the profile.

Before the program is run, starting values must be determined for M, $x_{1,p}$ $x_{2,p}$, $x_{3,p}$, $x_{4,p}$ and $x_{5,p}$. These start parameters can be estimated from a spectrum recorded simultaneously on a recorder or can be determined by a peak-find subroutine, which calculates them using the algorithms of Savitzky[42]. The former is to be preferred if the composition of the mixture is known, because the peak-find routine may introduce an erroneous number of bands, usually too large, due to the influence of spectral noise. Although an increase of the number of bands improves the fit, the result of the procedure will not conform to physical reality[43].

The iterative procedure is stopped by the program when the desired value of $\Phi$ is reached, or if the maximum number of iterations is exceeded. The output contains the final position, height, width and area of the computed, constituent bands. If the Gauss/Lorentz sum function is used two heights are obtained for each band, i.e. $x_1$ and $x_5$. These heights belong, respectively, to the Lorentzian and the Gaussian part of the band. A zero value for $x_1$ or $x_5$ means that

a pure Gaussian or a pure Lorentzian band is found.

Plots (on hard copy and on a videoscreen) are available to check the procedure. These plots show the original spectrum, the calculated bands, the sum spectrum of these bands and the difference between the measured and the finally calculated spectrum.

In addition to this basic program routines were developed to apply signal averaging and solvent band subtraction to the measured spectra.

### 5.3. Signal averaging

Signal averaging is a way to improve signal-to-noise ratios. If a number of n spectra, recorded successively, under completely identical conditions, is added, an improvement of the signal-to-noise ratio by a factor $\sqrt{n}$ will be found, provided the noise varies randomly. A requirement for a succesful application of this method is the reproducibility of the measurement, hence the sample must be in chemical equilibrium, no temperature or pressure fluctuations should occur, and - most important - no drift of the wavenumber scale should take place. The latter was checked by scanning the 546 nm (1123 $cm^{-1}$ in the Raman spectrum) atom line of Hg, produced by the fluorescent lamps in the laboratory ten times over a period of three hours. A maximum difference of 0.1 $cm^{-1}$ was found for the position of this band, which is tolerable.

A way to cope with a possible shift of the wavenumber scale is the introduction of a reference point for the absolute wavenumber in the separate spectra. As reference point the already mentioned Hg-line could be used. Before addition of the spectra, the position of the reference point in the separate spectra must be determined and, if necessary, the spectra must be shifted until all reference points coincide. Although the application of the shift procedure is easy, in practice it is hardly necessary, because the data acquisition can be started very reproducibly. Fig.7 shows the effect of signal averaging on the signal-to-noise ratio of the 1050 $cm^{-1}$ band of $NO_3^-$, for several values of n.

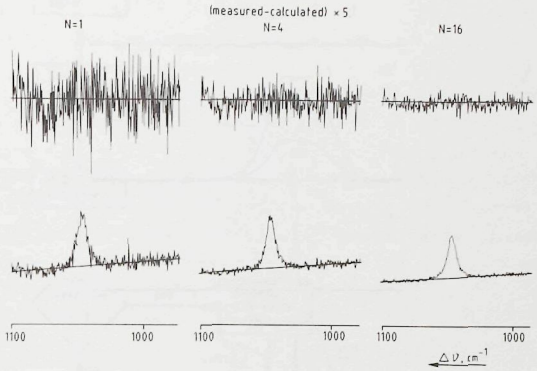


*Fig.7. Influence of signal averaging on the signal-to-noise ratio of the 1050 $cm^{-1}$ band of nitrate ($10^{-3}$ Mol.$l^{-1}$ in $H_2O$). N=1, no signal averaging, N=4 and N=16 addition of 4 and 16 spectra, respectively.*

### 5.4. Solvent band subtraction

Solvent bands or other species present in the mixture can give rise to background spectra. It can be advantageous to subtract this background before processing a band, or a band envelope. This is known as spectrum stripping.

First the spectrum of the mixture and the spectrum of the pure compound causing the background are recorded and stored in computer memory. To both spectra baseline correction is applied and from the spectrum of the mixture a spectral range is defined where only background bands are found. The multiplication factor is determined over this spectral range. Then the background spectrum is multiplied by the appropriate factor and subtracted, point by point, from the spectrum of the mixture. The resulting net spectrum is processed with the curve

fit program.

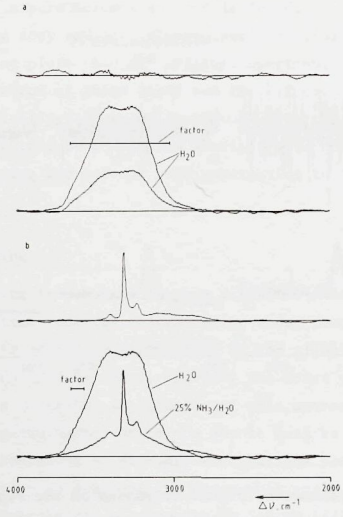


*Fig.8. Digital subtraction of the water band from (a) a water spectrum and (b) the spectrum of a 25% solution of ammonia in water. In (a) only noise remains after subtraction, in (b) an ammonia spectrum is found which is in good agreement with spectra reported in literature.*

It is obvious that again the wavenumber scales of the spectrum of the mixture and of the background spectrum must coincide. The procedure to check and correct a shift is identical to the method described earlier for signal averaging. In addition to the shift of the wavenumber scale, caused by instrumental factors the bands can also shift with respect to each other, due to temperature effects. Since temperature changes may also influence the width of Raman bands it is important to record the spectrum of the mixture and the background spectrum at the same temperature. Further, it is well known that Raman bands may have slightly different positions in different chemical environments. This has to be taken into consideration as well,



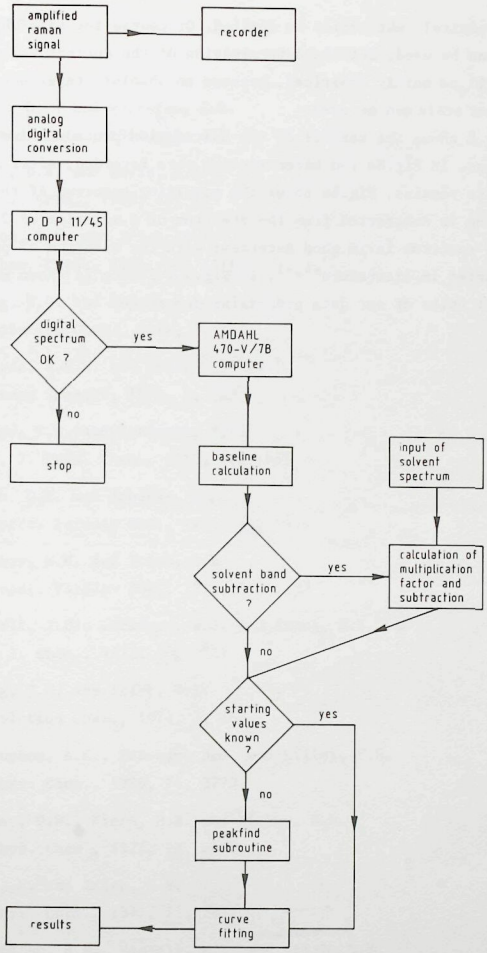


*Fig.9. Scheme of the data-processing.*

before spectral subtraction is applied. Of course the same shift procedure can be used, but the determination of the correct value for the shift will be mainly empirical, because no absolute reference for the wavenumber scale can be used.

Fig.8 shows the results of the subtraction procedure for two situations. In Fig.8a two water spectra were recorded; after subtraction only noise remains. Fig.8b shows the resulting spectrum if the water background is subtracted from the spectrum of a solution of 25% $NH_3$ in $H_2O$. The spectrum is in good agreement with the spectrum of pure ammonia reported in literature[44,45]. In Fig.9 a scheme is shown which contains all units of our data processing procedure.



REFERENCES


1. Irish, D.E. and Walrafen, G.E.
   J. Chem. Phys., 1967, 46, 378
2. Irish, D.E. and Davis, A.R.
   Can. J. Chem., 1968, 46, 943
3. Nelson, D.L. and Irish, D.E.
   J. Chem. Phys., 1971, 54, 4479
4. Chang, T.G. and Irish, D.E.
   J. Solution Chem., 1974, 3, 175
5. Edwards, H.G.M. and Woodward, L.A.
   J. Raman Spectr., 1974, 2, 423
6. Egorov, V.N. and Kuzinets, I.E.
   Russ. J. Phys. Chem., 1975, 49, 1688
7. Irish, D.E. and Brooker, M.H.
   Transact. Faraday Soc., 1971, 67, 1916
8. Brooker, M.H. and Irish, D.E.
   Transact. Faraday Soc., 1971, 67, 1923
9. Riddell, J.D., Lockwood, D.J. and Irish, D.E.
   Can. J. Chem., 1972, 50, 2951
10. Chang, T.G. and Irish, D.E.
    J. Solution Chem., 1974, 3, 161
11. Covington, A.K., Freeman, J.G. and Lilley, T.H.
    J. Phys. Chem., 1970, 74, 3773
12. Bonner, O.D., Flora, H.B. and Aitken, H.W.
    J. Phys. Chem., 1971, 75, 2492
13. Chen, H. and Irish, D.E.
    J. Phys. Chem., 1971, 75, 2672
14. Covington, A.K., Hassall, M.L. and Irish, D.E.
    J. Solution Chem., 1974, 3, 629
15. Covington, A.K. and Thompson, R.
    J. Solution Chem., 1974, 3, 603

16. Sze, Y.K. and Irish, D.E.
Can. J. Chem., 1975, 53, 427

17. Cunningham, K.M., Goldberg, M.C. and Weiner, E.R.
Anal. Chem., 1977, 49, 70

18. Meyer, B., Ospina, M. and Peter, L.B.
Anal. Chim. Acta, 1980, 117, 301

19. Stobbaerts, R.F., Van Haverbeke, L. and Herman, M.A.
J. Food Sci., 1983, 48, 521

20. Bus, J.
Anal. Chem., 1974, 46, 1824

21. Irish, D.E. and Riddell, J.D.
Appl. Spectrosc., 1974, 28, 481

22. Wancheck, P.L. and Wolfram, L.E.
Appl. Spectrosc., 1976, 30, 542

23. Gaber, B.P. and Peticolas, W.L.
Biochim. Biophys. Acta, 1977, 465, 260

24. Karvaly, B. and Loshchilova, E.
Biochim. Biophys. Acta, 1977, 470, 492

25. Bower, D.I. and Ward, I.M.
Polymer, 1982, 23, 645

26. Atalla, R.H.
Appl. Polym. Symp., 1983, 37, 295

27. Chang, R.K. and Benner, E.
Report US Gas Res. Inst. no. GRI-79/0050, 1979

28. Diller, D.E. and Chang, R.F.
Appl. Spectrosc., 1980, 34, 411

29. Setchell, R.E. and Ottesen, D.K.
Report Sandia Lab., Livermore USA no. Sand 74-8644, 1974

30. Seliskar, C.J., Spangler, P.A., Hale, M.D. and Rudy, C.R.
Appl. Spectrosc., 1983, 37, 77

31. Daigneault, G.R., Morris, M.D. and Schneggenburger, R.G.
Appl. Spectrosc., 1983, 37, 443



32. Long, M.B., Fourguette, D.E., Escoda, M.C. and Layne, C.B.
Opt. Lett., 1983, 8, 244

33. Placzek, G.
"Marx Handbuch der Radiologie", 1934, 6

34. Eckhardt, G. and Wagner, W.G.
J. Mol. Spectrosc., 1966, 19, 407

35. Kalashnikova, L.P. and Sidorov, N.K.
Opt. Spectrosc., 1970, 28, 260

36. Kalashnikova, L.P. and Sidorov, N.K.
Opt. Spectrosc., 1970, 29, 421

37. Koike, J., Suzuki, T. and Fujiyama, T.
Bull. Chem. Soc. Jpn., 1976, 49, 2724

38. Abe, N. and Ito, M.
J. Raman Spectrosc., 1978, 7, 161

39. Shorygin, P.P.
Zh. Fiz. Khim. SSSR, 1947, 21, 1125

40. Asthana, B.P. and Kiefer, W.
Verhandl. DPG. (VI), 1982, 17, 390

41. Pitha, J. and Jones, R.N.
NRC Bull. no. 12, National Research Council of Canada,
Ottawa Canada, 1968

42. Savitzky, A.
Anal. Chem., 1961, 33, 25A

43. Vandegiste, B.G.M. and De Galan, L.
Anal. Chem., 1975, 47, 2124

44. Schwartz, M. and Wang, C.H.
J. Chem. Phys., 1973, 59, 5258

45. Buback, M. and Schulz, K.R.
J. Phys. Chem., 1976, 80, 2478

# Chapter III A FEASIBILITY STUDY

## 1. Introduction

Many chemical processes proceed at non-ambient conditions of elevated temperature and pressure. The development and optimization of process conditions benefit from a knowledge of the exact composition of the reaction mixture. Normally this is achieved by sampling and off-line analysis. Circumstances are conceivable, however, where this technique fails and in-situ analysis must be used. An example is the synthesis of urea. Urea is formed in a two-step reaction:

$$2NH_3 + CO_2 \rightleftarrows H_2NCOONH_4 \qquad (1)$$

$$H_2NCOONH_4 \rightleftarrows H_2NCONH_2 + H_2O \qquad (2)$$

Normal synthesis conditions are $170 < T < 210^{o}$ C and $15 < p < 25$ MPa[1]. A change of pressure or temperature will give a considerable change of the composition of the reaction mixture. Hence, sampling and off-line analysis may produce unreliable results and in-situ analysis is to be preferred for the determination of all reaction components. For this purpose spectroscopic methods are suitable.

Common spectroscopic techniques cannot be used in this case. UV spectroscopy would give data for the carbonyl compounds and for ammonia, but not for water. By contrast, IR spectroscopy is impossible, because a major part of the spectrum will be obscured due to the presence of water in the mixture. Only Laser Raman Spectrometry (LRS) seems feasible. The visible radiation used to excite and detect Raman transitions can be easily directed to a measuring cell. Water is an acceptable solvent and all components, including water, give a characteristic Raman band.

The advantages of LRS for quantitative analysis have been shown for gases[2], liquids[3] and solids[4]. Better analytical results are to be expected if relative intensities are used instead of absolute ones, since Raman intensities are affected by many experimental factors[5,6,7]. The standard to which the intensities are related must be added to the mixture, since no solvent is used in the urea synthesis. The suggestion of Tunnicliff and Jones[8] to eliminate a number of the experimental

factors in quantitative Raman analysis by diluting the sample, cannot be used, if in-situ analysis is desired.

Generally, the Raman effect is weak and the detection limits are rather high. A significant improvement of the signal-to-noise ratio is possible, if multiple scan and signal averaging techniques are used. Another advantage of computerized data processing is the possibility of curve fitting, which is important in the case band overlap occurs.

In-situ analysis implies the need to study the influence of temperature and pressure[9] on the chemical composition. Before such conclusions can be drawn, it must be verified that the temperature and pressure have no, or a known influence upon the spectra produced by the components.

## 2. Experimental

### 2.1. Apparatus

The Raman spectrometer used for the experiments was composed of a scanning double grating monochromator, the Jobin Yvon Ramanor HG2S, with a Coherent CR-2 laser as light source. The 514.5 nm line of the Ar-ion laser at a power of 1 Watt was used. Detection was carried out photometrically using a Hamamatsu R 376 photomultiplier tube, a DC amplifier and a recorder. Integrated bandareas were measured with a Shimadzu Chromatopac CE1B integrator. The conventional 90° geometry was applied to collect the scattered radiation (Fig.1).

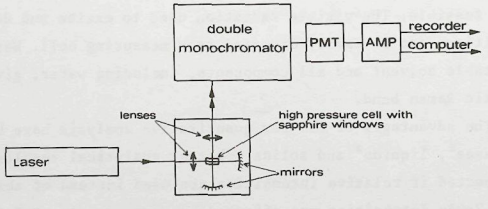


*Fig.1. The Laser Raman Spectrophotometer.*



### 2.2. The cells

Since Raman spectra are obtained in the visible part of the spectrum optical materials can be used that transmit radiation in this region. Hence, in most cases cells or cell windows of ordinary glass can be used. The experiments at atmospheric pressure and ambient or elevated temperatures were carried out in a cell entirely made of glass. The cell was heated electrically with resistance wire, the contents were stirred and the temperature was controlled with a thermocouple.

For the experiments at elevated pressure a Nova Swiss cell was used. This cell, suitable for pressures upto 400 MPa, has a stainless steel housing and three sapphire windows. Due to corrosian of the stainless steel housing the cell could not be used for mixtures containing ammonia. The pressure in the cell was generated hydraulically. Sapphire, like glass, has the quality of transmitting visible radiation, but it has a much higher resistance against corrosian and pressure. A disadvantage of sapphire is its birefringence, because the orientation of the windows may influence the polarization properties of the incident and scattered radiation and hence the intensity of some Raman bands.

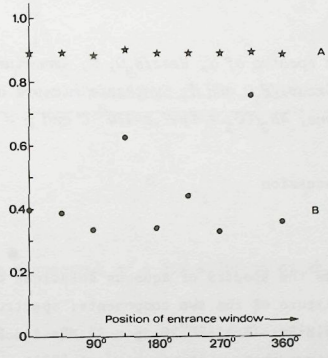


*Fig.2. Variation of the intensity ratios of $CCl_4$ bands with the position of the sapphire entrance windas of the high pressure cell. A, ratio $I_{CCl_4,220\ cm^{-1}}/I_{CCl_4,318\ cm^{-1}}$ and B, ratio $I_{CCl_4,220\ cm^{-1}}/I_{CCl_4,460\ cm^{-1}}$.*

Figure 2 shows the influence of the orientation of the entrance window on the intensity ratios of different $CCl_4$ bands. Since the 220 $cm^{-1}$ and the 318 $cm^{-1}$ bands have the same depolarization ratio[10] and are affected in the same way by the position of the entrance window, their intensity ratio remains constant. The 460 $cm^{-1}$ band however is completely polarized and rotation of the cell window changes the intensity of this band significantly, as is shown by the change of the ratio $I_{220\ cm^{-1}}/I_{460\ cm^{-1}}$.

To obtain reproducible results, it is, therefore, mandatory to ensure a fixed position of the sapphire cell windows.

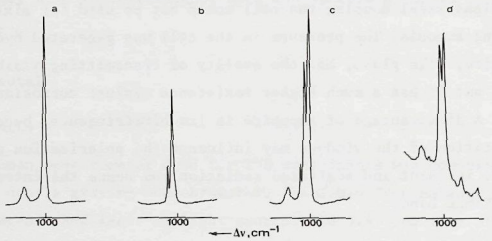


*Fig.3. Raman spectra of a, Urea/$H_2O$, b, Ammoniumcarbamate/$H_2O$, c, Mixture/$H_2O$ and d, Synthesis mixture at process conditions, $NH_3/CO_2$ = 2, T = 170° C and p = 25 MPa.*

## 3. Results and discussion

### 3.1. The spectra

Figure 3 shows the spectra of aqueous solutions of urea, ammoniumcarbamate and a mixture of the two components; spectrum D was made under process conditions (T = 170° C, p = 25 MPa and $NH_3/CO_2$ = 2). The carbamate spectrum shows a strong band at 1035 $cm^{-1}$ (C-N stretching), suitable for a quantitative determination. The shoulder at the high frequency side of this band does not arise from carbamate, but from carbonate[11], formed in the reaction of carbamate with water. A band at the low frequency side, at 1020 $cm^{-1}$, would indicate the presence



of bicarbonate. These bands will probably be absent under the very strong alkaline conditions that prevail during the urea synthesis. The Raman spectrum of urea is well-known[12,13]. It has a strong band at 1005 $cm^{-1}$ (C-N stretching) and although this band overlaps partially with the 1035 $cm^{-1}$ band of carbamate both bands can be readily determined with computerized data processing. The very broad band in these spectra, situated in the 3000-3600 $cm^{-1}$ region, can be assigned to the OH-stretching vibrations[14] of the water that was used as a solvent. Superimposed on this band are some weak bands that can be assigned to the N-H stretching vibrations[14] of urea and carbamate.

*These features are also encountered in the spectrum of a 25% aqueous solution of ammonia (Fig.4). Besides the bands assigned to the O-H and N-H stretching vibrations this spectrum shows weak bands at 1100 $cm^{-1}$ and 1650 $cm^{-1}$, arising from the bending vibrations of* $NH_3$[15,16,17] and $H_2O$, respectively.

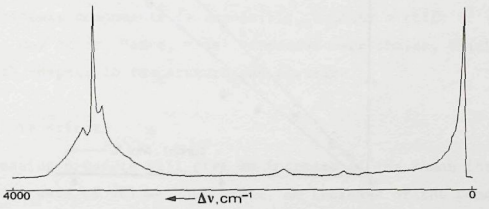


*Fig.4. Raman spectrum of a 25% solution of $NH_3$ in $H_2O$.*

Carbondioxide is a three atomic molecule with a centre of symmetry and hence the Raman spectrum should only show one band, assigned to the symmetrical C-O stretching vibration[14]. This very strong band is situated at 1388 $cm^{-1}$. Due to Fermi resonance a second band is present however at 1286 $cm^{-1}$.

3.2. Analytical characteristics

The absolute intensity of a Raman band can be given by

$$I = A \cdot \Omega \cdot L \cdot [C] \qquad (3)$$

where A is a constant, $\Omega$ is the Raman scattering cross section, L is the factor for the local field correction[18] and [C] is the concentration of the scattering compound. Hence, absolute intensities will be directly proportional to the concentration only if A, $\Omega$ and L are independent of the concentration.

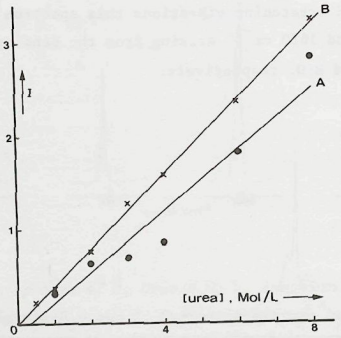


*Fig.5. Intensity of the 1005 $cm^{-1}$ band of urea vs. the concentration of urea, A for the absolute intensity and B, for the intensity of the urea band relative to the intensity of the 920 $cm^{-1}$ band of ACN, added as internal standard.*

Fig.5 shows the intensity of the 1005 $cm^{-1}$ band of urea in aqueous solution as a function of the concentration, with and without the addition of acetonitrile (ACN) as internal standard. It is obvious that the absolute intensity values show a strong scatter, mainly due to cell repositioning.



If relative intensities are used in stead of absolute intensities, the coefficient of variation for each individual point, found with repetitive scans, is considerably larger; 5% in stead of 3%. Since the points lie much closer to a straight line however, ACN appears to be effective as internal standard. The detection limits based on a signal-to-noise ratio of 2, for urea and ammoniumcarbonate in aqueous solution are $4.10^{-3}$ and $5.10^{-3}$ $mol.L^{-1}$ respectively. For the present purpose these figures are adequate, since at process conditions the carbamate formation proceeds to completion and 50 to 80% of the carbamate is converted to urea[1].

3.3. Quantitative analysis at non-ambient conditions

The above data were obtained at atmospheric pressure and ambient temperature. The synthesis of urea however proceeds at elevated pressure and temperature and therefore calibration at ambient conditions and extrapolation to process conditions is only possible if the effect of p and T on the spectra is analysed. A direct study of these effects on the synthesis components is impossible, because a shift of the equilibria may occur. Hence, model compounds were chosen, which are stable with respect to temperature and pressure.

3.4. Pressure effects

Increasing pressure will give an increase of the Raman intensities, due to a decrease of volume, and hence, an increase of the concentration. This effect will be very pronounced for gases, less for liquids and negligible for solids, due to the difference in compressibility. If only the compressibility is taken into account molar intensities remain constant and an internal standard eliminates the effect of compression.

Literature data indicate that a change of pressure may result in a shift of the Raman frequencies[19,20], while no change of the molar intensities is observed. If the change of pressure however causes a change of the polarizability tensor a significant effect, not only on the frequency, but also on the molar intensity may be expected. This appears to be the case for liquid and fluid ammonia[15]. The effect of pressure found for this compound was explained by assuming that the pyramidal height of the $NH_3$ molecule is sensitive to pressure changes.

A change of the pyramidal height results in a change of the polarizability tensor and hence in a change of the molar scattering intensity. This effect turns out to be different at different temperatures.

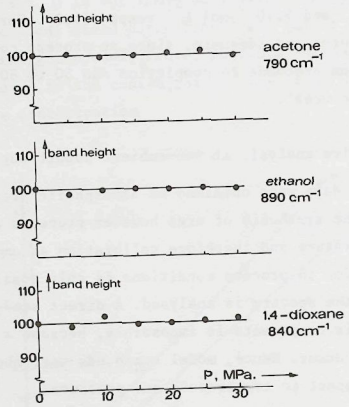


*Fig.6. Variation of the Raman band heights of some model compounds with pressure.*

Fig.6 shows the effect of pressure on the intensity of bands of pure ethanol, acetone and 1,4-dioxane. A correction was made for the increase of intensity due to compression, approximately 3% in the range from 0.1 to 30 MPa at 293 K.

The figure shows that up to 30 MPa the pressure does not affect the Raman intensities of these bands. Neither was a change of band frequencies observed. Hence, the exceptional behaviour found for ammonia[15] is not encountered for these compounds, nor is it expected for a compound like urea.

### 3.5. Temperature effects

The factors that have to be taken into account if the effect



of temperature on the intensity of Raman bands is considered are

- thermal expansion
- local field effect
- population factors
- polarizability- and hyperpolarizability tensor

It is obvious that thermal expansion will lead to a decrease of the observed Raman intensities, due to a decrease in concentration. The appropriate correction is simple and is required only if absolute intensities are measured. Relative intensities, ratioed to an internal standard, are not affected by thermal expansion, since the change in concentration is equal for the compound to be measured and the standard.

The correction factor the local field effect will also be influenced by a change of temperature, since the index of refraction is a function of the temperature. According to Eq.(II-3), for pure water a decrease of the Raman intensity of 5% will be found if the temperature increases from 293 K to 373 K. If the assumptions made to derive Eq.(II-4) are valid, the intensities of all Raman bands will be influenced to the same extent. Hence the use of an internal standard compensates for thermal expansion as well as for the change of the correction factor for the local field effect.

The temperature enhancement of the intensity of Stokes Raman bands, due to a change of the population factors, is given by[21]

$$\frac{I(T)}{I(T_o)} = \frac{1 - \exp(-hcv_r/kT_o)}{1 - \exp(-hcv_r/kT)} \qquad (4)$$

where $v_r$ is the Stokes Raman shift and h, c and k are fundamental physical constants. This equation predicts that the increase of I with T is more pronounced as the band lies closer to the Rayleigh band. For example, the intensity of a band at 3000 $cm^{-1}$ increases by less than 0.1% if the temperature increases from 293 to 523 K, whereas a band at 1000 $cm^{-1}$ would increase by 6%. Relative intensities are affected too, since the band of the standard must have a Raman shift different from that of the compound which has to be measured. In all cases, however, this effect can be easily calculated and the appropriate correction applied.

The Raman scattering cross section of a band is a function of the polarizability and the hyperpolarizability[22]

$$\Omega = C \cdot (B + A \cdot \bar{F}) \qquad (5)$$

where B is a function of the polarizability tensor only and A is a function of the polarizability - and the hyperpolarizability tensor. $\bar{F}$ is the averaged electric field operating on the scattering molecule and caused by the electric field of all molecules present in the solution. Since $\bar{F}$ is a function of the temperature, $\Omega$ will also be a function of temperature. The significance of this effect is determined by the magnitude of $A \cdot \bar{F}$, which depends on the hyperpolarizability of the scattering compound and on the dipole moments of solvent and solutes and their concentrations. This effect is difficult to predict and must be analysed experimentally.

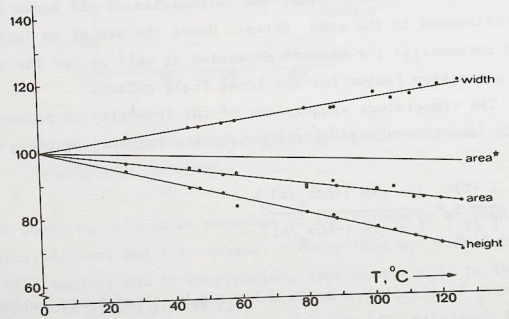


*Fig.7. Variation of the band parameters of the 1020 $cm^{-1}$ band of 1,2-dichlorobenzene with temperature. Area★ is the measured area, corrected for thermal expansion.*

Except for the population factor, all factors mentioned will result in a decrease of the absolute Raman intensity with increasing temperature.



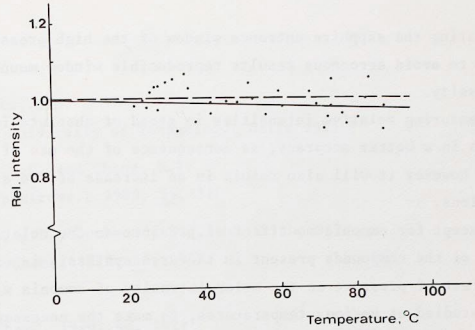


*Fig.8. Variation of the ratio $I_{urea,1005\ cm^{-1}}/I_{ACN,920\ cm^{-1}}$ with temperature. The drawn line was calculated through the points, the broken line is found if a correction is applied for the variation of the population factors with temperature.*

Fig.7 shows the effect of temperature on the band parameters of the 1020 $cm^{-1}$ band of 1,2-dichlorobenzene. An increase of the bandwidth is found with increasing temperature. This is no compensation however for the decrease of the integrated area. This decrease in intensity is predictable, since the concentration decreases by approximately 11% due to thermal expansion over the range from 273 K to 373 K and the population factor increases by less than 1%. In Fig.8 the effect of temperature on the relative intensity of the 1005 $cm^{-1}$ band of urea in an aqueous solution is shown. ACN was used as internal standard. A decrease of the relative intensity of 3.5% is found in the range from 273 K to 373 K. Due to the population factors of urea and ACN a decrease can be predicted of 1%. Hence, 2.5% must be attributed to a change of the ratio $\Omega_{urea}/\Omega_{acn}$, since the influence of the local field effect and the thermal expansion are eliminated.

## 4. Conclusions

Raman intensities are affected by a number of instrumental and fundamental factors. The use of an internal standard may compensate for many of the instrumental factors, but not for all, as was shown

by rotating the sapphire entrance window of the high pressure cell. Hence, to avoid erroneous results reproducible window mountings are a necessity.

Measuring relative intensities in stead of absolute intensities results in a better accuracy, as consequence of the use of a scanning system however it will also result in an increase of the standard deviations.

Except for ammonia no effect of pressure on the relative intensities of the compounds present in the urea synthesis is expected. The effect of pressure on the molar intensity of ammonia will have to be studied at various temperatures, to make the necessary corrections possible. A new cell will be designed, enabling us to do measurements at process conditions, without having corrosion or polarization problems.

All bands in the spectrum of the mixture will be affected by temperature. Partially this effect will be reduced by the use of an internal standard, but corrections have to be made for example for the population factor.

Laser Raman Spectrometry seems feasible for quantitative, in-situ analysis of the urea synthesis mixture at process conditions, if irreproducebility due to trivial instrumental factors is avoided, if a proper internal standard is used and if the necessary corrections for the temperature effect - and in the case of ammonia for the pressure effect - are made.



REFERENCES


1. Lemkowitz, S.M.
   Thesis, University of Technology, Delft 1975

2. Diller, D.E. and Chang, R.F.
   Appl. Spectrosc., 1980, 34, 311

3. Riddell, J.D., Lockwood, D.J. and Irish, D.E.
   Can. J. Chem., 1972, 50, 2951

4. Bus, J.
   Anal. Chem., 1974, 46, 1824

5. Bernstein, H.J. and Allen, G.
   J. Opt. Soc. Am., 1955, 45, 237

6. Long, D.A., Milner, D.C. and Thomas, A.G.
   Proc. Roy. Soc. London, 1956, 237A, 197

7. Rea, D.G.
   J. Opt. Soc. Am., 1959, 49, 90

8. Tunnicliff, D.D. and Jones, A.C.
   Spectrochim. Acta, 1962, 18, 579

9. Irish, D.E., Jary, T. and Ratcliffe, C.I.
   Appl. Spectrosc. 1982, 36, 137

10. Murphy, W.F., Evans, M.V. and Bender, P.
    J. Chem. Phys., 1967, 47, 1836

11. Oliver, B.G. and Davis, A.R.
    Can. J. Chem., 1973, 51, 698

12. Saito, Y., Machida, K. and Uno, T.
    Spectrochim. Acta, 1971, 27a, 991

13. Duncan, J.L.
    Spectrochim. Acta, 1971, 27a, 1197

14. Herzberg, G.
    "Infrared and Raman Spectra of Polyatomic Molecules".
    Van Nostrand, New York, 1945

15. Buback, M. and Schulz, K.R.
    J. Phys. Chem., 1976, 80, 2478

16. Gardiner, D.J., Hester, R.E. and Grossman, W.E.L.
J. Raman Spectrosc., 1973, 1, 87

17. Schwartz, M. and Wang, C.H.
J. Chem. Phys., 1973, 59, 5258

18. Eckhardt, G. and Wagner, W.G.
J. Mol. Spectrosc., 1966, 19, 407

19. Walrafen, G.E.
J. Chem. Phys., 1971, 55, 5137

20. Whalley, E.
Proc. 4th Int. Conf. on High Pressure, Kyoto, Japan, 1974

21. Placzek, G.
"Marx Handbuch der Radiologie", 1934, 6

22. Koike, J., Suzuki, T. and Fujiyama, T.
Bull. Chem. Soc. Jpn, 1976, 49 2724



## Chapter IV MEASUREMENTS AT PROCESS CONDITIONS

### 1. Introduction

Urea, the world's most important nitrogeneous fertilizer, is commercially produced via two reversible and independent reactions occuring in a heterogeneous system:

$$2(NH_3)_G + (CO_2)_G \rightleftarrows (H_2NCOONH_4)_L \quad (1)$$

$$(H_2NCOONH_4)_L \rightleftarrows (NH_2CONH_2)_L + (H_2O)_L \quad (2)$$

in which the subscripts G and L refer to the gas and liquid phase, respectively. Normal synthesis conditions are $170 < T < 210^{\circ}$ C and $15 < p < 25$ MPa. Sampling for analysis purposes is far from simple due to the difficult conditions prevailing, namely high temperatures and pressures, the extremely corrosive nature of the liquid phase and the strong tendency of the liquid to change significantly upon lowering its temperature and pressure, i.e. upon bringing it to ambient conditions. Published analytical results are based exclusively on batch experiments carried out in autoclaves. Since sizable samples are usually withdrawn, normally only one composition at one given temperature can be measured per batch filling. It is for these reasons that few experimental data are available in the literature. These data and the description of the tedious experimental techniques used are found in a number of publications[1-4]. It should further be remarked that these data mainly describe urea conversions; the unconverted carbon dioxide is assumed to exist only in the form of ammonium carbamate.

Sampling difficulties can be circumvented by an in situ analytical technique. In a previous study we discussed the feasibility of Laser Raman Spectrometry (LRS) for the quantitative analysis of the urea synthesis solution under process conditions of high temperature and pressure[5]. It was shown that characteristic vibrational bands for all reaction components can be found in three regions of the Raman spectrum; these are presented in Table 1. The influence of the temperature and the pressure upon the Raman band paramaters was investigated in experiments with model compounds. It was concluded that the use of

Laser Raman Spectroscopy (LRS) might well be feasible for quantitative in situ analysis of the urea synthesis solution. In this study we will demonstrate that, at least over a certain composition range, LRS can be used to determine the concentration of urea and other chemical constituents under process conditions.

| Range, $cm^{-1}$ | Species | Type of Vibration | Band position, $cm^{-1}$ |
|---|---|---|---|
| 900 - 1100 | Urea | $\nu_{C-N}$ | 1005 |
| | Amm.carbamate | $\nu_{C-N}$ | 1035 |
| 1200 - 1400 | Carbon dioxide | Fermi.res. | 1286 |
| | Carbon dioxide | $\nu_{C-N}$ | 1388 |
| 2800 - 3800 | Ammonia | $\nu_{N-H}$ | Several bands from 3100 - 3400 |
| | Water | $\nu_{O-H}$ | Broad combination band from 2900 - 3600 |

*Table 1. Strongest bands of the main species present in the urea synthesis solution. Wavenumbers shown for ambient temperature.*

## 2. Experimental

### 2.1. Instrumentation

The optical components used to record the Raman Spectra have been described previously[5]. We also stressed the need for a sample cell that allows measurements at temperatures and pressures typical for the urea synthesis and that withstands the corrosive reaction mixture.

Fig.1 shows the cell used in this study. The optical part is made of synthetic sapphire, used because of its excellent strength and corrosion resistance. The cell was fabricated by Saphirwerk AG Nidau in Switzerland. The cell-housing is made of titanium alloy (6% Al, 4% V), The cell and its housing were designed by Durisch[6].



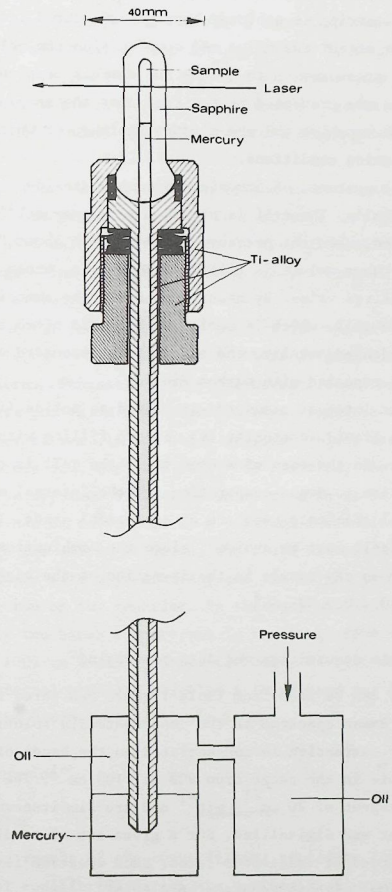


*Fig.1. The high pressure Raman cell.*

The pressure in the cell is generated hydraulically with oil, the sample is separated from the oil by means of mercury. The cell is placed in an air oven taken from a Perkin Elmer gas chromatograph. Sample stirring is achieved by a glass-covered iron stirrer, activated by a magnet moving up and down outside the cell. The cell has been used at pressures up to 35 MPa and temperatures up to 520 K. Corrosion problems are prevented by the fact that the sample is only in contact with the sapphire and the mercury, neither of which is attacked at the reaction conditions.

The mixtures of ammonia and carbon dioxide are prepared gas volumetrically. The cell is attached to a gas-rack[7] and the assembly is evacuated. When the pressure is reduced to about 0.004 Pa, a container with a known volume is filled with ammonia, whose pressure is adjusted to a desired value. By means of mercury the ammonia is then displaced into the cell, which is cooled with liquid nitrogen. After the ammonia has condensed totally, the assembly is evacuated again and the procedure is repeated with carbon dioxide.

The internal standards are added as solids (in the case of salts) or as a liquid (acetonitrile), before filling with ammonia and carbon dioxide. In the case of acetonitrile the cell is cooled during the evacuation to avoid evaporation of the internal standard.

All chemicals used are of analytical grade. The presence of oxygen in the cell must be avoided, since the combination of ammonia, mercury and oxygen can result in the formation of the highly explosive Million's base $(HO)_2\ Hg_2\ NH_2\ OH$[8].

## 2.2. Data acquisition and data processing

As can be seen from Table 1 there are three ranges of interest in the Raman spectrum of the urea synthesis solution. In this study, however, attention is concentrated on the bands of urea and ammonium carbamate in the range from 900 to 1100 $cm^{-1}$. The spectra are scanned with a speed of 20 $cm^{-1} \cdot min^{-1}$ and are simultaneously recorded on a recorder and digitalized. For a given set of conditions the spectrum is recorded at least four times. Each spectrum is started at the same wavenumber with an accuracy of 0.1 $cm^{-1}$.

The data acquisition is carried out by means of a PDP 11/45 computer at a rate of 0.78 Hz. This means that the signal is sampled every



0.427 $cm^{-1}$ and that 468 data points are available over a spectral range of 200 $cm^{-1}$. The digitized spectrum is checked for errors which might have occured during the data acquisition process. For this purpose a program (ASPECT) is available on the PDP 11/45 that displays the digitized spectrum on the videoscreen of a Tektronix 4006-1, where it can be compared with the spectrum that is recorded simultaneously on the recorder. When no errors are detected the spectrum is transmitted to the University's central Amdahl 470-V/7B computer, which processes the data.

The first step of the data processing is the improvement of the signal-to-noise ratio by signal averaging four or more spectra recorded under identical conditions. The second step is the calculation of a baseline as a straight line through the first and the last 25 data points in the spectral range.

The main part of the program used to process the spectra consists of the program developed by Pitha and Jones[9]. This program fits, in an iterative procedure, combinations of Gauss-Lorentz funtions through the experimental data points. A fixed Gauss-Lorentz ratio is chosen in advance. The other parameters for which starting values are required are the number of bands and, for each band, the position, the height and the width. If the spectrum of an unknown mixture is to be fitted the starting values can be determined by a peakfind subroutine. In the present study, where the sample is known, the width and position of each band can be stated with high accuracy and the height can be estimated from the spectrum on the recorder. In the case of the urea synthesis solution only two bands are present in the range from 900 to 1100 $cm^{-1}$: urea at 1005 $cm^{-1}$ and ammonium carbamate at 1035 $cm^{-1}$. Depending on the internal standard selected a third band may be present, but its band parameters are again known.

# 3. Results and discussion

## 3.1. Signal processing

Fig.2 shows the result of the curve-fitting procedure for spectra recorded at chemical equilibrium during the synthesis of urea, at $L = 5$, $W = 0$, where L and W are the molar $NH_3/CO_2$ and $H_2O/CO_2$ ratio, respectively, and $p = 30.0$ MPa at two different temperatures. It is clear that the two adjacent bands of urea (990 $cm^{-1}$) and carbamate

(1025 $cm^{-1}$) are incompletely resolved. The spectrum is complicated further by the presence of a third band at 1045 $cm^{-1}$ that belongs to nitrate added as internal standard. The necessity of this choice will become clear below. The difference spectrum also shown in this figure demonstrates that a good fit is obtained.

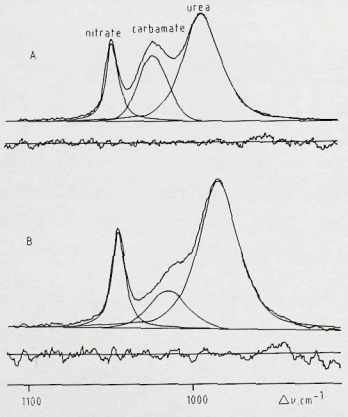


*Fig.2. Raman spectrum and difference spectrum of urea synthesis solution at: (a) p = 30.0 MPa, L = 5, W = 0 and T = 127°C (b) p = 30.0 MPa, L = 5, W = 0 and T = 203°C*

Fig.3 shows the improvement obtained by signal averaging. The reduction in peak to peak noise in the difference spectrum by a factor of two agrees well with the expectation for random noise. Table 2 demonstrates that signal averaging introduces no errors in the band parameters. Indeed the mean bandarea and bandwidth calculated from four to six separately processed spectra are equal to the bandarea and bandwidth found from the signal averaged spectrum.

In our previous study we used stable model compounds to analyse the influence of temperature and pressure on the Raman band parameters.



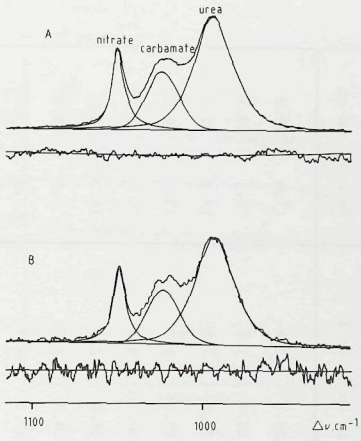


*Fig.3. Improvement obtained by signal averaging:*
*(a) recorded 4 times at p = 30.0 MPa, T = 141°C, L = 5 and W = 0*
*(b) recorded once at p = 30.0 MPa, T = 141°C, L = 5 and W = 0*

Over the range of interest in the urea synthesis no pressure influence was observed. The temperature influence depends on the nature of the compounds and the Raman band considered. Generally a temperature increase of 100° C shifts the band to lower wavenumber, decreases the bandheight (up to 15%) and increases the bandwidth (up to 15%). However, after correction for expansion, the bandareas are found to be constant to within 3% and thus provide an excellent measure of the concentration. Because the composition of the urea synthesis solution changes with temperature, it is not possible to analyse a change of intrinsic band areas with temperature for the compounds presently investigated. However, indirect evidence for a similar behaviour of

| Number of spectra | Temperature in °C | Separately processed: Band Area in A.U. | Separately processed: Standard deviation in % | Separately processed: Band Width in $cm^{-1}$ | Separately processed: Standard deviation in % | Signal averaged: Band Area in A.U. | Signal averaged: Band Width in $cm^{-1}$ |
|---|---|---|---|---|---|---|---|
| 4 | 145 | 17.9 | 2.7 | 28.4 | 2.4 | 17.9 | 28.2 |
| 4 | 155 | 16.8 | 1.4 | 28.9 | 1.6 | 17.3 | 29.1 |
| 4 | 172 | 17.2 | 3.3 | 28.8 | 1.9 | 17.3 | 29.1 |
| 4 | 186 | 12.7 | 2.2 | 29.5 | 1.8 | 13.1 | 30.0 |
| 4 | 196 | 14.6 | 1.6 | 30.2 | 0.5 | 14.4 | 30.1 |
| 5 | 150 | 14.3 | 2.3 | 29.0 | 2.5 | 14.3 | 28.9 |
| 5 | 201 | 8.8 | 3.2 | 29.9 | 2.6 | 8.8 | 29.8 |
| 6 | 162 | 14.5 | 6.2 | 29.3 | 4.9 | 14.5 | 29.2 |
| 6 | 182 | 15.7 | 2.4 | 29.1 | 1.5 | 15.8 | 29.2 |

*Table 2. Influence of signal averaging on the band parameters of the 1005 $cm^{-1}$ band of urea.*



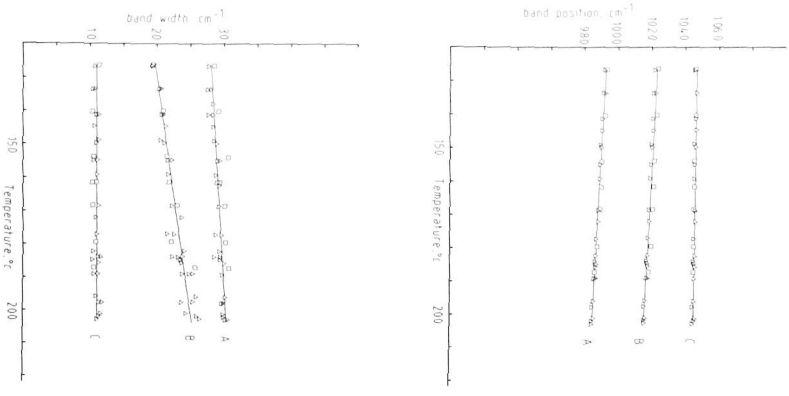


*Fig. 4. Influence of temperature on band position (top) and band width (bottom) of A, urea, B, carbamate and C, nitrate (Δ L = 5 and □L = 3).*

the urea synthesis solution compounds with respect to the model compounds can be derived from the variations of peak position and bandwidth presented in Fig.4. Indeed, the shifts to lower wavenumber observed for nitrate (2 $cm^{-1}$), carbamate (8 $cm^{-1}$) and urea (9 $cm^{-1}$) are quite normal, apart from the fact that these shifts do not affect the measurement of the bandareas. Similarly, the increases in bandwidth by 25% for carbamate and 9% for urea agrees well with the result found for the model compounds. Consequently, by correspondence we presume that over a range of 100° C the band areas of the compounds involved in the urea synthesis (notably urea itself) provide a reliable measure for their concentrations.

### 3.2. The internal standard

In our preliminary study the favourable influence of an internal standard upon the analytical accuracy was reported. We concluded that its use compensates for instrumental factors, like laser instability and for fundamental factors, like thermal expansion. In the present study several internal standards were tested at high temperature and pressure in a mixture of ammonia and carbon dioxide.

Acetonitrile, ammonium sulfate and ammonium thiocyanate all have strong free-lying bands, but were insuitable, because they are insoluble or decompose in the reaction mixture.

Good results were obtained with nitrate, which proved to be stable and soluble at all temperatures and pressures. Nitrate, added in the form of potassium nitrate, has a very strong Raman band at 1050 $cm^{-1}$ (at ambient temperature), arising from the symmetrical N-O stretching vibration. Fig.2 shows that it is sufficiently resolved from the carbamate band to allow its quantification with the curve-fitting program. Fig.5 shows an experiment (L = 5, W = 0 and p = 30.0 MPa) in which nitrate (8% by weight) was used as an internal standard. The total experiment lasted over a month. The pressure was kept constant over this period and the temperature was varied randomly. The measurements were carried out at chemical equilibrium. The figure shows that the wide scattering found for the absolute area of carbamate band significantly decreases if the area is measured relative to the area of the nitrate band.



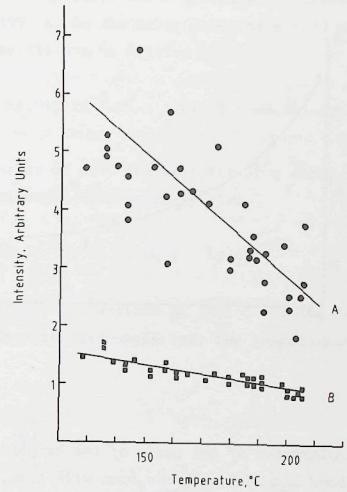


*Fig.5. Intensity of the carbamate band vs. temperature at p = 30.0 MPa, L = 5, and W = 0. A, absolute intensity, and B, intensity relative to the intensity of the nitrate band.*

### 3.3. Conversion measurements

In the following section the experimental results will often be compared to the value found with the most recent equation for the conversion of carbon dioxide to urea. According to Gorlovskii and Kucheryavyi[10] this equation for the liquid phase is:

$$X_G(L,W.T) = 94.31\ L - 139.9\ L^{0.5} - 4.284\ L^2 - 26.09\ W + 2.664\ WL + 1.54\ T - 0.09346\ TL - 1.059\ 10^{-5}\ T^3 - 97.82 \quad (3)$$

where X is the conversion of inital carbon dioxide to urea in mol%, L is the inital molar ratio $NH_3/CO_2$, W is the initial molar ratio

$H_2O/CO_2$ and T is the temperature in $^oC$.

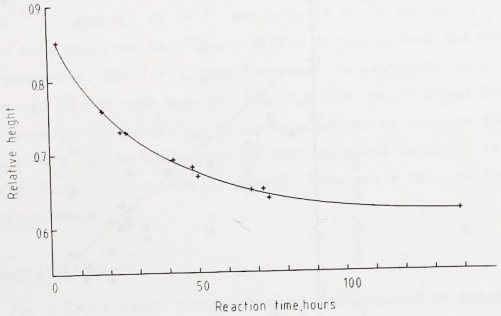


*Fig.6. Relaxation of the ratio of the heights of the urea band and the carbamate band with time, for p = 25.0 MPa, L = 2 and W = 0. At time zero the temperature is dropped from 180 to 95° C.*

Fig.6 shows the ratio of the heights of the urea and the carbamate band as a function of time for p = 25.0 MPa, L = 2 and W = 0. In this experiment the temperature was first kept at 180° C for 24 hours and was then decreased to 95° C, whereupon the ratio of the peak heights was measured as a function of time. No internal standard is needed for such relative data. The figure shows that it takes almost a week before equilibrium is reached at this, for urea synthesis, very low temperature.

In Fig.7 the relative intensity of the urea band is shown as a function of temperature for two different sets of conditions. Nitrate was used as internal standard, and all points were measured after equilibrium had been reached, which takes about five hours at 150° C and less than one hour at 200° C. In this figure the solid curves have been calculated after Eq.(3) with an appropriate scaling factor. It is seen that the experimental results follow the expression of



Gorlovskii and Kucheryavyi very well. Indeed, for p = 25 MPa, L = 3 and W = 0 (curve A) Eq.(3) predicts a continuous increase of the urea band up to 199° C. On the other hand, at p = 30 MPa, L = 5 and W = 0 (curve B) Eq.(3) can be written as

$$X_G(5,0,T) = -1.059\ 10^{-5}\ T^3 + 1.073\ T - 46.20 \qquad (4)$$

with a scaling factor of 21.0 the best fit of a similar function through the experimental data points yields

$$X_{Exp} = -1.089\ 10^{-5}\ T^3 + 1.100\ T - 49.47 \qquad (5)$$

Both expressions reach a maximum at 184° C and the difference between Eqs.(4) and (5) is within 0.5 mol% over the temperature range of 120 to 210° C.

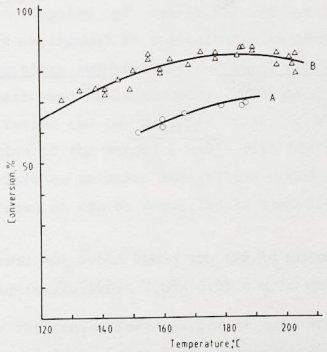


*Fig.7. Conversion of carbon dioxide to urea as a function of the cell temperature for A, p = 25.0 MPa, L = 3 and W = 0, and B, p = 30.0 MPa, L = 5 and W = 0. Solid lines were calculated after Eq.(4); the experimental data points were scaled to fit at T = 150° C.*

Fig.5 shows that under these conditions the relative intensity of the carbamate band decreases continuously. Up to 184° C this decrease can be attributed to the decreased formation of urea. However, for temperatures over 184° C both the carbamate and urea band in the liquid phase decrease. As expected, no urea was found in the gas phase, but both ammonia and carbon dioxide were found (Fig.8). Apparently, at high temperature the carbamate decomposes by the reverse reaction of Eq.(1).

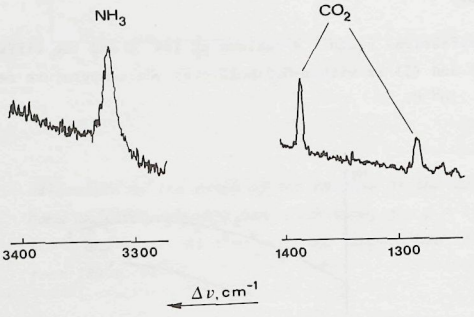


*Fig.8. Spectrum of the gas phase above the urea synthesis solution at p = 30.0 MPa, T = 215° C, L = 5 and W = 0.*

### 3.4. Calibration

So far no absolute urea concentrations have been measured, since a reproducible calibration in the sapphire cell was not yet possible. This problem is due to the birefringence[5] of the sapphire, which causes a change of the molar intensities of the Raman bands if the position of the cell is changed, which occurs when the cell is removed for cleaning and refilling. During one series of measurements,



however, the cell stays in a fixed position and hence the molar Raman intensities do not change during the experiment, as can been seen from Fig.7. Fig.7 also shows that one single reference point suffices to calculate the urea concentration at all conditions during the experiment. The calibration problem, inherent in the use of sapphire as cell material, does not occur if a glass cell is used, since glass shows no birefringence. Glass, however, is less strong and corrosion resistant than sapphire, but can be used in experiments of short duration at moderate temperatures and pressures. We therefore suggest the calibration to be carried out as follows.

First the intensity of the urea band is measured in aqueous solution as a function of the concentration at ambient temperature and pressure in a glass cell, using nitrate as internal standard. Then the glass cell is filled with a mixture of ammonia, carbon dioxide and nitrate, and the equilibrium relative intensity of urea is measured at moderate temperature (T < 150°) and pressure (p < 10 MPa), giving the urea concentration at a given p, T, L and W. Subsequently the experiment in the sapphire cell can be carried out at identical values for L and W. This experiment is started with an equilibrium measurement at the temperature and pressure for which the calibration in the glass cell was performed. This procedure provides the relation between the urea concentration and the relative intensity measured for this particular position of the sapphire cell. With the result of this measurement all further relative intensities found at different temperatures and pressures can be converted to concentrations, for this given experiment.

## 4. Discussion and conclusions

Compared to the conventional method of urea analysis, i.e., taking samples from an autoclave, Laser Raman spectrometry offers the great advantage that any number of measurements can be performed with one filling without changing its composition. This advantage makes LRS eminently suitable for the study of solution composition as a function of temperature, pressure and time.

A number of problems reported in our previous article has been solved. Potassium nitrate was found to be a suitable internal standard, being stable and soluble over the temperature range of 120° to

210° C. Its presence corrects well for day-to-day fluctations of instrumental factors like laser power and amplification. Adequate data processing techniques have also been developed. A remaining problem is the birefringence of sapphire, for which the internal standard does not correct. Rather than attempting highly reproducible cell positioning, we propose indirect calibration with corresponding solutions in a glass cell.

At a composition of L = 5 (molar) and W = 0 a comparison of the experimental results for the urea conversation obtained with LRS showed good agreement with conversions calculated using the expression of Gorlovskii and Kucheryavyi[10].

Despite the good agreement, however, we should be cautious in drawing general conclusions concerning the applicability of LRS for quantitative analysis of urea solutions. In processing the Raman bands we have ignored the possible presence of ammonium bicarbonate. This assumption is necessary, since, as we reported in our previous article, the Raman bandsof urea (1005 $cm^{-1}$) and bicarbonate (1018 $cm^{-1}$) overlap to such a degree that they cannot be resolved with the present curve-fitting program.

The absence of a carbonate band at 1065 $cm^{-1}$ is an indication, but no guarantee, that the bicarbonate concentration is negligible at our experimental conditions. Unfortunately, beyond measurements of urea conversions no analytical data concerning the urea solution exists nor do molecular-thermodynamic models which succesfully describe the phase equilibria of the synthesis solution shed any light on this question, since these models explicidly assume that carbamate is the sole ionic species present in the solution[11]. Models applied to more dilute urea synthesis solutions ($H_2O/CO_2 > 1$) at much lower temperature do account for the formation of bicarbonate[12,13]. In fact these models predict substantial bicarbonate concentrations, $HCO_3^-/NH_2COO^- > 1$.

These composition predictions, however, have never been checked with direct, analytical measurements of the ionic species present, nor is it clear to what extent these models can be used in the range of the urea synthesis conditions. It is obvious that further experiments are necessary to determine the general applicability of Laser Raman Spectrometry to analysis of the urea synthesis solution.



REFERENCES


1. Kawasumi, S.
   Bull. Chem. Soc. Japan, 1951, 24, 148; 1952, 25, 227; 1953, 26, 218; 1954, 27, 254

2. Gorlovskii, D.M., Gorbushenkov, V.A. and Kucheryavyi, V.I.
   Zhurn. Prikl. Khim., 1972, 45, 1533

3. Inoue, S., Kanai, K. and Otsuka, E.
   Bull. Chem. Soc. Japan, 1972, 45, 1339

4. Durisch, W., Buck, A.,Lemkowitz, S.M. and Van den Berg, P.J.
   Chimia, 1979, 33, 293

5. Van Eck, M., Van Dalen, J.P.J. and De Galan, L.
   Analyst, 1983, 108, 485 (Chapter III of this thesis)

6. Durisch, W.
   Personal communication

7. Lemkowitz, S.M.
   Ph.D. Thesis, University of Technology, Delft, 1975

8. Michels, A.M.J.F., Dumoulin, E.M.L. and Gerver, J.H.
   Rec. Trav. Chim. 1957, 76, 6

9. Pitha, J. and Jones, R.N.
   NRC Bulletin no.12, National Research Council of Canada, Ottawa 1968

10. Gorlovskii, D.M. and Kucheryavyi, V.I.
    Zhurn. Prikl. Khim., 1980, 53

11. Van Krevelen, D.W. Hoftijzer, P.J. and Huntjens, F.J.
    Recueil, 1949, 68, 191

12. Newman, S.A.
    Thermodynamics of Aqueous Systems with Industrial Applications, A.C.S. Symposium Series 133, 1980, G. Maurer, 139

13. Kotula, E.
    J. Chem. Techn. Biotechnol., 1981, 31, 103

## Chapter V THE BICARBONATE CONCENTRATION

### 1. Introduction

In the previous chapter we compared our analytical results to conversions calculated with the equation of Gorlovskii and Kucheryavyi[1]. We concluded that, at least for L = 5 and W = 0, good agreement is found. We also stated that the method is generally applicable only if the bicarbonate concentration in the solution is negligible, since our curve-fit program cannot fit Raman spectra of solutions containing urea and bicarbonate simultaneously. This is due to the fact that the line separation between urea (1005 $cm^{-1}$) and bicarbonate (1018 $cm^{-1}$) is too small to be distinguished by the program.

However, some reaction models[2,3] predict substantial concentrations of bicarbonate in urea synthesis solutions and, in fact, consider bicarbonate as an intermediate in the formation of carbamate. According to these models the formation of carbamate from bicarbonate proceeds as

$$NH_3 + HCO_3^- \rightleftarrows NH_2COO^- + H_2O \qquad (1)$$

It is, therefore, interesting to consider the presence of bicarbonate in aqueous solutions of ammonia and carbon dioxide, in the absence of urea.

Since there will always be a considerable amount of carbamate in such solutions, the conditions, i.e. temperature and pressure, must be chosen such that no urea is formed, in order to enable the determination of the bicarbonate concentration. For sufficiently low temperatures ($t < 100^{\circ}$ C) the rate of the dehydratation reaction of carbamate to urea, Eq.(2), will be low enough to prevent interfering urea concentrations.

$$H_2NCOOCH_4 \rightleftarrows H_2NCONH_2 + H_2O \qquad (2)$$

When no urea is allowed to be formed, the formation of water is also excluded. However, bicarbonate can only be formed from carbon dioxide in the presence of water. For this reason our model studies of the equilibrium between carbamate and bicarbonate are carried out in

aqueous solutions.

The reverse reaction of Eq.(1) is the hydrolysis of the carbamate ion. The reaction, which benefits from a low pH, can easily be observed at ambient temperature and pressure by measuring the Raman spectrum of aqueous solutions of ammonium carbamate. Three bands are found in the range from 1000 to 1100 $cm^{-1}$, a $HCO_3^-$ band at 1018 $cm^{-1}$, a carbamate band at 1035 $cm^{-1}$ and a $CO_3^{2-}$ band at 1065 $cm^{-1}$. It is found that the relative intensity of the carbamate band decreases with time, whereas the intensities of the $HCO_3^-$ and $CO_3^{2-}$ bands increase. Eventually, at even lower pH, in an open system all carbon containing species will disappear from the solution according to the reactions[4]

$$CO_3^{2-} + H^+ \rightleftarrows HCO_3^- \quad , pK_a = 10.3 \tag{3}$$

$$HCO_3^- + H^+ \rightleftarrows CO_2 + H_2O \quad , pK_a = 6.4 \tag{4}$$

Indeed, when hydrochloric acid is added to the carbamate solution, gas bubbles appear and, in the Raman spectrum of the solution, no bands are found in the range from 1000 to 1100 $cm^{-1}$. Relatively stable ammonium carbamate solutions can only be obtained by raising the pH to pH > 14.

## 2. Experimental

In chapter III we already described the optical components used to measure the Raman spectra. Unlike the measurements in the previous chapter, the measurements described here were performed at moderate temperatures and pressures ($t < 100^{\circ}$ C and $p < 5$ MPa), so it was not necessary to use the high pressure sapphire cell. The cell used in this part of the study was made of a capillary glass tube. The inner diameter of the cell was 4 mm, with 2.5 mm wall thickness. The use of the glass cell avoids cell positioning problems.

The pH was measured with a pH-meter of the type Metrohm Herisau E520, using a glass electrode. The pH was adjusted to the desired value by adding aqueous solutions of potassium hydroxide or hydrochloric acid. The Raman spectra of the solutions were measured after the pH had stabilized. After recording the spectrum the pH was measured again and if the difference was greater than 0.05 pH units, the procedure was repeated.



3. Measurements on aqueous solutions of ammonia and carbon dioxide, with and without the addition of an internal standard.

### 3.1. Introduction

The addition of an internal standard enables the calculation of absolute quantities of carbamate and bicarbonate from the measured Raman intensities, by using the molar intensities relative to the internal used. The relative molar intensities are obtained by measuring the Raman spectra of solutions with known concentrations of carbamate and standard or bicarbonate and standard. As standard the nitrate ion was used, which was added as potassium nitrate.

First the molar intensity of the 1065 $cm^{-1}$ band of carbonate was determined relative to the intensity of the 1050 $cm^{-1}$ band of $NO_3^-$, from the spectrum of a solution with known concentrations $K_2CO_3$ and $KNO_3$. It was verified that no bicarbonate band was present, and, from the measured intensities and the known concentrations, the constant ratio $I_{CO_3^{2-}} \cdot [NO_3^-] / I_{NO_3^-} \cdot [CO_3^{2-}]$ was calculated.

The determination of the calibration factor for $HCO_3^-$ was carried out with an aqueous solution of $KHCO_3$ and $KNO_3$. Besides the bands of $HCO_3^-$ and $NO_3^-$ at 1018 and 1050 $cm^{-1}$, respectively, a third band was found at 1065 $cm^{-1}$, showing the presence of carbonate in the solution. Hence, the concentration $HCO_3^-$ could not be calculated straightforward from the amount of $KHCO_3$ which was used. Therefore, we first determined the $CO_3^{2-}$ concentration from the 1065 $cm^{-1}$ band. The initial amount $KHCO_3$ was corrected for this concentration and the ratio $I_{HCO_3^-} \cdot [NO_3^-] / I_{NO_3^-} \cdot [HCO_3^-]$ was calculated. The procedure was checked by converting all $HCO_3^-$ to $CO_3^{2-}$ using potassium hydroxide. From the relative intensity of the resulting $CO_3^{2-}$ band the carbonate concentration was calculated. Comparison of this concentration with the initial amount of $KHCO_3$ showed an error of less than 2 percent.

To determine the relative molar intensity of the 1035 $cm^{-1}$ band of the carbamate ion, ammonium carbamate and potassium nitrate were dissolved in an aqueous solution of potassium hydroxide with a pH > 14. Three bands were found in the Raman spectrum of the solution: a small $CO_3^{2-}$ band at 1065 $cm^{-1}$, the nitrate band at 1050 $cm^{-1}$ and a carbamate

band at 1035 $cm^{-1}$. After applying the appropriate correction for the presence of $CO_3^{2-}$, the calibration factor for carbamate was calculated relative to $NO_3^-$.

| | $I_{Sp} \cdot [NO_3^-] / I_{NO_3^-} \cdot [Sp]$ | |
|---|---|---|
| Species | This study | Cunningham et.al.[5] |
| $NO_3^-$ | 1 | 1 |
| $CO_3^{2-}$ | 0.36 | 0.38 |
| $HCO_3^-$ | 0.22 | 0.21 |
| $H_2NCOONH_4$ | 0.52 | - |

*Table 1. Relative molar Raman intensities of the constituents of aqueous solutions of ammonium carbamate, using $NO_3^-$ as internal standard.*

In table 1 the results of the calibration are shown. The values found for the molar intensity ratios of $HCO_3^-$ (1018 $cm^{-1}$) and $CO_3^{2-}$ (1065 $cm^{-1}$) relative to the molar intensity of $NO_3^-$ (1050 $cm^{-1}$) are in good agreement with the results of Cunningham *et.al.*[5], which are also listed in the table.

3.2. Results and discussion on the measurements with addition of potassium nitrate

In table 2 the results are given of measurements on the system $NH_3/CO_2/H_2O/NO_3^-$, as a function of the temperature at a constant pressure of 5.0 MPa. The initial molar ratios $NH_3/CO_2$ and $H_2O/CO_2$ were 5.0 and 1.5, respectively. The figures for band width and band area found in this table result from the curve-fit procedure; from the band areas we calculated the amounts of carbamate and bicarbonate, which are found in Table 3. As an example, Fig.1 shows the spectrum measured at 85° C.



| Time at equilibrium, hours | Temperature, °C | Area, arbitrary units | | | Area, relative to $A_{NO_3^-}$ | | Width, $cm^{-1}$ | | |
|---|---|---|---|---|---|---|---|---|---|
| | | $HCO_3^-$ | $H_2NCOONH_4$ | $NO_3^-$ | $HCO_3^-$ | $H_2NCOONH_4$ | $HCO_3^-$ | $H_2NCOONH_4$ | $NO_3^-$ |
| 14 | 85 | 3.94 | 14.47 | 6.21 | 0.63 | 2.35 | 22.8 | 18.1 | 8.7 |
| 18 | 96 | 4.33 | 10.37 | 5.63 | 0.77 | 1.84 | 27.2 | 17.5 | 10.0 |
| 2 | 63 | 4.43 | 12.02 | 5.75 | 0.77 | 2.09 | 24.8 | 16.9 | 8.9 |
| 7 | 63 | 4.45 | 12.04 | 5.83 | 0.76 | 2.07 | 25.1 | 16.9 | 9.0 |
| 1 | 102 | 5.23 | 9.52 | 5.19 | 1.01 | 1.83 | 32.1 | 17.7 | 9.5 |
| 2 | 102 | 5.95 | 9.28 | 4.90 | 1.21 | 1.89 | 35.8 | 17.7 | 9.3 |
| 2 | 73 | 6.00 | 10.57 | 4.97 | 1.21 | 2.13 | 35.7 | 17.4 | 8.6 |
| 4 | 73 | 5.69 | 10.56 | 5.17 | 1.10 | 2.04 | 34.3 | 17.4 | 8.9 |
| 6 | 73 | 5.55 | 10.50 | 5.23 | 1.06 | 2.01 | 34.0 | 17.2 | 8.7 |
| 7 | 73 | 5.36 | 10.80 | 5.12 | 1.05 | 2.11 | 34.4 | 17.4 | 8.8 |
| 21 | 73 | 3.78 | 8.95 | 4.27 | 0.89 | 2.10 | 33.4 | 17.6 | 8.8 |
| 24 | 73 | 4.52 | 8.35 | 4.34 | 1.04 | 1.92 | 32.2 | 17.0 | 8.4 |
| 29 | 73 | 7.13 | 13.65 | 6.00 | 1.19 | 2.28 | 36.0 | 17.9 | 8.4 |

*Table 2. Chronologically ordered results of measurements on a $NH_3/CO_2/H_2O/NO_3^-$ system. Initial molar ratios $NH_3/CO_2$ and $H_2O/CO_2$ are 5.0 and 1.5, respectively. Initial molar quantities of carbon dioxide and potassium nitrate were 0.54 and 0.055 mmol, respectively. The measurements were performed at a constant pressure of 5.0 MPa.*

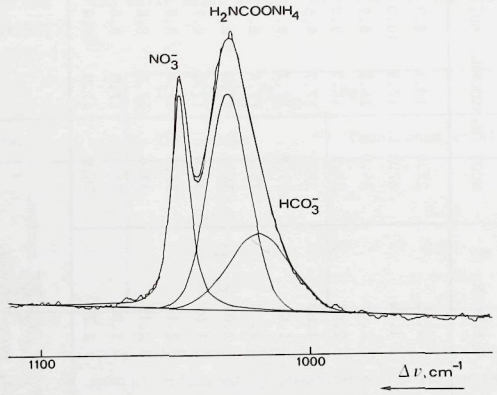


*Fig.1. Raman spectrum of an aqueous solution of ammonia and carbon dioxide, recorded at 85° C and 5 MPa. Initial molar ratios $NH_3/CO_2$ and $H_2O/CO_2$ were 5.0 and 1.5, respectively. $KNO_3$ was added as internal standard.*

If all carbon dioxide reacts to either carbamate or bicarbonate, the total mole sum of carbamate and bicarbonate should equal the initial molar quantity of carbon dioxide, as can be seen from the reactions

$$CO_2 + H_2O + NH_3 \rightleftarrows HCO_3^- + NH_4^+ \quad (5)$$

$$CO_2 + 2NH_3 \rightleftarrows H_2NCOO^- + NH_4^+ \quad (6)$$

It is clear from Table 3 that discrepancies are found at all temperatures. A maximum deviation of 31% was found at 96° C. A possible explanation might be presence in the solution of other species that have consumed carbon dioxide. Free carbon dioxide is not very likely, considering the ample excess of ammonia. Indeed, no bands were found indicating its existence. No band was found at 1065 $cm^{-1}$, the position



of the carbonate band, either.

| Temperature, °C | Area relative to $A_{NO_3^-}$ | | Calculated amount, mmol | | Total of carbon containing species, mmol |
|---|---|---|---|---|---|
| | $HCO_3^-$ | $H_2NCOONH_4$ | $HCO_3^-$ | $H_2NCOOCH_4$ | |
| 85 | 0.63 | 2.35 | 0.15 | 0.25 | 0.40 |
| 96 | 0.77 | 1.84 | 0.18 | 0.19 | 0.37 |
| 63 | 0.77 | 2.08 | 0.18 | 0.22 | 0.40 |
| 102 | 1.11 | 1.86 | 0.26 | 0.20 | 0.46 |
| 73 | 1.08 | 2.08 | 0.25 | 0.22 | 0.47 |
| | | | | initial $CO_2$ | 0.54 |

*Table 3. Amounts of carbamate and bicarbonate calculated from the results in Tables 1 and 2, compared to the initial amount of carbon dioxide (0.54 mmol).*

If we consider the data in Table 2, which are ordered chronologically, we observe that the width of the $HCO_3^-$ band is initially around 25 $cm^{-1}$, but increases to over 32 $cm^{-1}$ from the measurement at 102° C on. No decrease of the band width was found when the temperature was lowered to 73° C, which justifies the assumption that no longer one band was present at the position of the bicarbonate band, but two. This second band could be due to urea, although its formation at 102° C is unlikely. Moreover, this would not explain the difference in the mass balance, found initially at 85° C.

A possible reason for the disagreement might be that the curve-fit program makes an incorrect assessment of the weaker shoulder band of bicarbonate (see Fig.1). To analyse this possibility further it was found advantageous to remove the disturbing influence of the nitrate band.

### 3.3. Results and discussion on the experiments without the use of an internal standard

Table 4 lists the results of measurements on the system $NH_3/CO_2/H_2O$ as a function of the temperature, at a constant pressure of 3.0 MPa.

| Time at equilibrium, hours | Temperature, °C | Area, arbitray units | | Width, $cm^{-1}$ | | $A_{HCO_3^-}/A_{H_2NCOONH_4}$ fit with variable positions | | $A_{HCO_3^-}/A_{H_2NCOONH_4}$ fit with fixed positions | |
|---|---|---|---|---|---|---|---|---|---|
| | | $HCO_3^-$ | $H_2NCOONH_4$ | $HCO_3^-$ | $H_2NCOONH_4$ | ratio | sd, % | ratio | sd, % |
| 24 | 85 | 4.71 | 7.04 | 30.6 | 14.4 | 0.67 | 38 | 0.13 | 5 |
| 4 | 95 | 2.38 | 7.30 | 27.9 | 18.4 | 0.33 | 12 | 0.14 | 0 |
| 3 | 61 | 2.59 | 8.18 | 23.4 | 16.9 | 0.32 | 25 | | |
| 14 | 61 | 1.80 | 6.35 | 22.6 | 17.1 | 0.28 | 9 | | |
| 19 | 61 | 3.36 | 7.77 | 25.6 | 15.7 | 0.43 | 60 | 0.14 | 3 |
| 50 | 88 | 2.14 | 8.15 | 23.2 | 17.6 | 0.26 | 4 | 0.14 | 3 |
| 24 | 71 | 3.01 | 7.26 | 27.2 | 16.4 | 0.41 | 93 | | |
| 50 | 71 | 1.74 | 8.33 | 23.2 | 17.6 | 0.21 | 7 | 0.15 | 3 |
| 24 | 83 | 2.26 | 8.49 | 26.6 | 18.1 | 0.27 | 38 | 0.15 | 8 |

*Table 4. Chronologically ordered results of measurements on a $NH_3/CO_2/H_2O$ system. Initial molar ratios $NH_3/CO_2$ and $H_2O/CO_2$ were 4.9 and 8.5, respectively. The measurements were performed at a constant pressure of 3.0 MPa.*



The initial molar ratios $NH_3/CO_2$ and $H_2O/CO_2$ were 4.9 and 8.5, respectively. The data found in this table are the average of the curve-fit results of four spectra, recorded within a short interval at constant temperature. As no internal standard was added, it was not possible to set up a mass balance.




*Fig.2. Raman spectra of an aqueous solution of carbon dioxide and ammonia, recorded in rapid succession under identical conditions: t = 85° C and p = 3 MPa. Initial ratios $NH_3/CO_2$ and $H_2O/CO_2$ were 4.9 and 8.5, respectively.*

Columns 7 and 8 show that for most measurements considerable standard deviations, up to 93%, are found for the mean value of the bicarbonate/carbamate intensity ratio. These deviations can be explained if we consider Fig.2, which shows two spectra recorded in rapid succession under identical conditions, and fitted with the same starting parameters. Although the spectra are identical, except for small random noise, the

curve-fit program finds two different values for the respective height, width and position of the two bands. Apparently the program fails to find a uniform solution for spectra that overlap too much.

As can be seen from Fig.2, the most obvious reason for this problem is the inability of the program to find the correct band positions. Hence, more reproducible curve-fit results are expected if the band positions are determined beforehand and if these positions are fixed during the iterative procedure.

The positions of the bicarbonate band and the carbamate band were determined relative to the position of the nitrate band at ambient temperature. From the values found for $\nu_{NO_3^-} - \nu_{HCO_3^-}$ and $\nu_{NO_3^-} - \nu_{H_2NCOO^-}$ the mutual distance $\nu_{H_2NCOO^-} - \nu_{HCO_3^-}$ was calculated to be 17 $cm^{-1}$. The curve-fit program was adapted to allow variation of the band positions, while keeping there mutual distance at this constant value. The effect of this procedure on the ratio of the areas is found in the last two columns of Table 4. It is clear that the standard deviations are now decreased to less than 10%. It also shows that the differences which are found between the ratios at different temperatures, are less than the standard deviation.

From the mean value of 0.14 for the ratio $A_{HCO_3^-}/A_{H_2NCOO^-}$ we can calculate, by means of Table 1 a concentration ratio bicarbonate/carbamate of approximately 0.3. As this result is much higher than expected, it gives rise to further investigation of the shape of the carbamate band, because even a slight asymmetry of the carbamate band on the low frequency side would give a considerable change of the ratio $A_{HCO_3^-}/A_{H_2NCOO^-}$ .

### 3.4. Conclusion

From the previous measurements the conclusion can be drawn that an accurate determination of the amounts of bicarbonate and carbamate in $NH_3/CO_2/H_2O$ solutions is not possible with the curve-fit program, if all curve-fit parameters are allowed to vary freely during the iterative procedure. Standard deviations up to 93% were found this way for the bicarbonate/carbamate intensity ratio. It was concluded that the program fails to find the correct band positions for spectra that show too much overlap. When the spectra were computed with a fixed value for the mutual distance between the carbamate band and the bicarbonate band, a more uniform curve-fit result was obtained and a clear improvement of the standard deviations to less than 10% was found.



As the value of 0.3 found for the bicarbonate/carbamate concentration ratio is much higher than expected for conditions of $NH_3/CO_2$ = 4.9, $H_2O/CO_2$ = 8.5, p = 3.0 MPa and $61^{\circ}$ C < t < $95^{\circ}$ C, we still doubt the accuracy of the result.

The most plausible reason for this deviation is an incorrect assumption with regard to the symmetry of the carbamate band. During the curve-fit procedure only two symmetrical bands were used, and, no eventual asymmetry of the bands was taken into consideration. The carbamate band and the bicarbonate band strongly overlap on the low frequency side of the carbamate band. Therefore, even a slight asymmetry of the carbamate band on the low frequency side would significantly influence the derived bicarbonate/carbamate intensity ratio. Hence, a further study on the shape of the carbamate band is necessary.

## 4. A study on the shape of the 1035 $cm^{-1}$ band of carbamate

### 4.1. Introduction

Band shapes and band widths in Raman spectroscopy are determined by the lifetimes of the molecular states involved in the transition. In general, the profile of a Raman band is a Voigt function, and, hence, the band should be symmetrical. Distortions of the profile are possible, however. Asymmetry may be caused by a number of instrumental and fundamental factors.

A plausible instrumental factor would be an aberration of the monochromator. Although an aberration might vary across the spectrum, we have no indication that our equipment will cause a measurable distortion of the carbamate band profile, because several symmetrical bands were found in the range from 900 to 1100 $cm^{-1}$, for instance, the band resulting from the symmetrical stretching vibration $\nu_{N-O}$ of nitrate at 1050 $cm^{-1}$.

A fundamental reason for the assymmetry of a Raman band would be the presence of isotopes, because the frequency of a vibration is mass dependent. The more pronounced the mass differences are, the

larger the separation between the isotope bands will be. For carbamate no significant isotope effects are expected, because the natural abundance of the uncommon isotopes of carbon, hydrogen, nitrogen and oxygen is very small[4].

Another fundamental origin of the asymmetry of a Raman band of a condensed sample may be an asymmetric distribution of the rotational levels over the vibrational band. Unlike the situation in gas phase spectra, the rotational fine structure is unresolved, but the vibration-rotation band contour is found to be asymmetrical. On the other hand, the same band in the solid sample will be symmetrical, because of the absence of rotations in the solid state. Anharmonicity of the vibration may also lead to an asymmetric band profile. In that case an asymmetric Raman band is found in the spectra of the gas, liquid and solid[6].

Finally, the presence of a side- band with a Raman shift close, but not equal to 1035 $cm^{-1}$, arising either from another carbamate vibration, or from the vibration of a carbamate-like species in the solution, may also cause an asymmetrical band contour. Infrared studies of solid ammonium carbamate at low temperatures show no evidence for the presence of a second band, however[7,8].

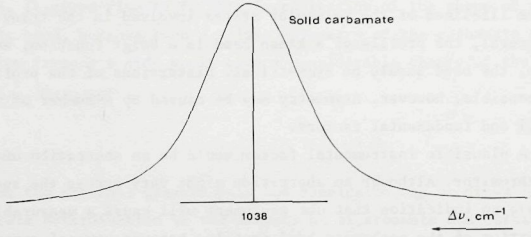


*Fig.3. The Raman band of solid ammonium carbamate found at 1038 $cm^{-1}$. The Δν - axis was extended to show the symmetry of the band.*



4.2. Aqueous carbamate solutions

In Fig.3 the band of solid ammonium carbamate is shown, which is found at 1038 $cm^{-1}$. It is obvious that this band is completely symmetrical. Hence, at least for the solid state, the conclusion can be drawn that the 1038 $cm^{-1}$ band of ammonium carbamate arises from a harmonic vibration, and no second band is present close to 1038 $cm^{-1}$.

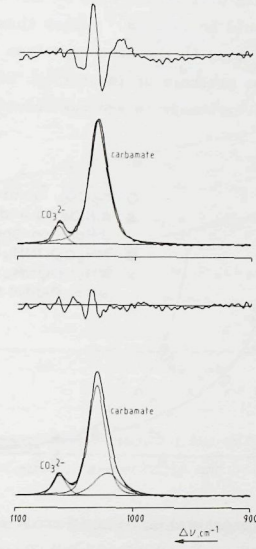


*Fig.4. The Raman spectrum of an aqueous solution of ammonium carbamate at pH > 14. The spectrum was fitted in two ways. The upper part shows a fit with two symmetrical bands, the lower part shows a fit with three symmetrical bands. It is evident from the difference spectra that the third band gives a clear improvement of the fit.*

Fig.4 shows the spectrum of an aqueous solution of ammonium carbamate at pH > 14. The spectrum was fitted in two ways. The upper part of the figure shows a fit with two symmetrical bands, one at 1065 $cm^{-1}$, the position of the carbonate band, and one at 1035 $cm^{-1}$, the position of the carbamate band. The lower part shows a fit with three symmetrical bands. From the difference spectra it is evident that the third band is necessary to obtain a good fit. The third band is situated at approximately 1025 $cm^{-1}$. It is unlikely that this band can be attributed to bicarbonate, because at pH = 14 the area of the bicarbonate band should be less than 0.1% of the area of the carbonate band and, moreover, its shift should be 1018 $cm^{-1}$ rather than 1025 $cm^{-1}$. The absence of the 1025 $cm^{-1}$ band in the Raman spectrum of solid ammonium carbamate rules out the presence of impurities. We conclude, therefore, that the Raman band of carbamate in aqueous solution is asymmetric.

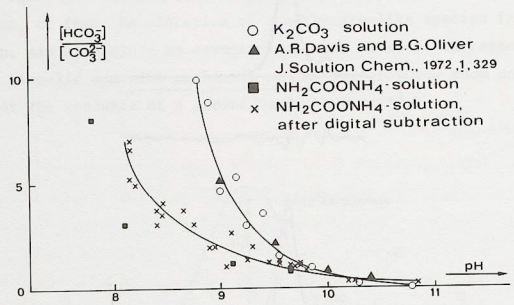


*Fig.5. The bicarbonate/carbonate concentration ratio as a function of the pH in aqueous solutions of $K_2CO_3$ and ammonium carbamate.*

A further indication for the asymmetry of the carbamate band, in aqueous solution, can be derived from the results in Fig.5. This figure shows the concentration ratio $HCO_3^-/CO_3^{2-}$ as a function of the pH. In the absence of carbamate this ratio was measured in aqueous solutions of potassium carbonate, and, as expected, the experimental results agree with theory and with results of Davis and Oliver[9], also



obtained by Raman spectroscopy.

In the presence of carbamate the results were calculated by fitting the spectra with three symmetrical bands. The position of the bicarbonate band was coupled to that of the carbonate band during the fit procedure. For that purpose the frequency difference of these bands was determined as a function of temperature in acidic, aqueous solutions of potassium carbonate. In Fig.6 this difference in Raman shifts is shown as a function of the temperature.

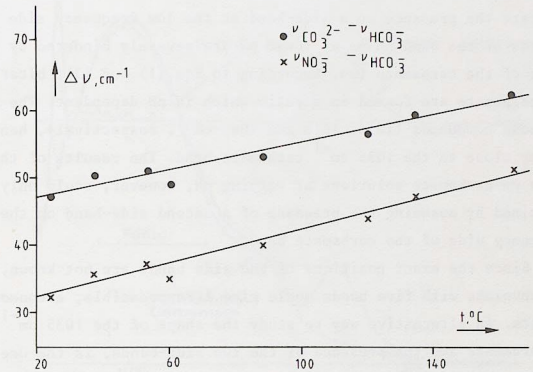


*Fig.6. The influence of temperature on the difference in Raman shifts for bicarbonate/carbonate and bicarbonate/nitrate.*

As can been seen from Fig.5, the fitting with three symmetrical bands leads to erroneous results for the bicarbonate/carbonate concentration ratio. Somewhat surprisingly, however, the ratio is generally found to be lower than the theoretical prediction. An ignored asymmetry of the carbamate band on the low frequency side would manifest itself by too high values for the bicarbonate/carbonate ratio, rather than the too low values found. This result can only be explained by the assumption that, in addition to the side-band at the low frequency side of the carbamate band, another side-band is present at the high frequency side. The position of this band must be close to

that of the carbonate band at 1065 $cm^{-1}$.

In view of Fig.5, the influence of the side bands on the $HCO_3^-/CO_3^{2-}$ ratio depends on the pH of the solution. At approximately pH < 10 the ratio is determined mainly by the side band at the high frequency side, as indicated by the too low values found, whereas at pH > 10 the influence of the low frequency side-band dominates, which is shown by the too high values for the $HCO_3^-/CO_3^{2-}$ ratio over this range.

The problem in studying the symmetry of the 1035 $cm^{-1}$ band of carbamate in aqueous solutions is caused basically by the instability of the carbamate ion. Relatively stable carbamate solutions, at pH > 14, indicate the presence of a side-band at the low frequency side (Fig.4). Studies of the band shape at lower pH are severely hindered by hydrolysis of the carbamate ion. According to Eqs.(1) and (3), bicarbonate and carbonate are formed in a ratio which is pH dependent. The bands of these compounds lie at 1018 and 1065 $cm^{-1}$, respectively, hence, rather close to the 1035 $cm^{-1}$ carbamate band. The results of the measurements on carbamate solutions at varying pH, however, could only be explained by assuming the presence of a second side-band on the high frequency side of the carbamate band.

Since the exact positions of the side bands are not known, fitting the envelope with five bands would give irreproducible, erroneous results. An alternative way to study the shape of the 1035 $cm^{-1}$ band of carbamate and the presence of the two side-bands, is the use of non-aqueous solvents. As no hydrolysis can occur in these solutions, the contours of the carbamate band and its side-bands, will not be obscured by the presence of bicarbonate or carbonate bands.

### 4.3. Non-aqueous carbamate solutions

Many liquids were examined as a possible solvent for ammonium carbamate. Acetone, acetonitrile, dimethylformamide, dimethylsulfoxide, 1,4-dioxane, ethanol and methanol were not suitable, either because the solvent does not dissolve ammonium carbamate sufficiently, or because the carbamate band completely disappears under a Raman band of the solvent. A solvent that satisfies the conditions is formamide.

In Fig.7 the spectra of formamide and of a solution of ammonium carbamate in formamide are shown; the spectra were recorded at ambient temperature and pressure. It is seen that the carbamate band is



situated on the flank of a formamide band. This poses no problem, however, bacause the computer program enables us to subtract the solvent spectrum from the combined carbamate/formamide spectrum. Previously, a multiplication factor must be determined to correct for instrumental variations in laser intensity and amplification and for the difference in the solvent concentration. The range where the multiplication factor was determined is shown in Fig.7.

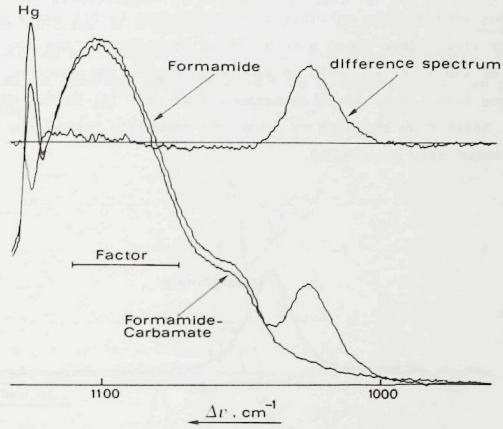


*Fig.7. The Raman spectra of formamide and of a solution of ammonium carbamate in formamide. The difference spectrum remains after digital subtraction of the formamide band from the combined spectrum.*

A closer examination of the figure shows that the solvent band in the combined spectrum is shifted with regard to the same band in the pure formamide spectrum. This shift of approximately 1 $cm^{-1}$ is not due to an inaccuracy in the experimental procedure, as can be seen from the identical positions of the Hg-line in the two spectra. The shift of the solvent band, under influence of the dissolved solute,

may lead to an incorrect subtraction procedure, as is shown by the calculated difference spectrum. On the left side of the carbamate band the difference spectrum intersects the zero axis; this intersection is found at the position of the formamide band in the original spectrum. This observation provides a simple means to correct for this shift by moving the digitized spectra point-by-point with regard to each other until the correct shift is found.

The difference spectrum calculated this way is shown in Fig.8, together with the best possible fit with one symmetrical band. Although the measured and the calculated spectrum seem to fit quite well, a closer view indeed shows a very slight asymmetry on the low wavenumber side of the band. As could be seen from Fig.4, the spectrum of an aqueous solution of ammonium carbamate at pH > 14, fitted with only one band, apart from the 1065 $cm^{-1}$ band of carbonate, shows the same phenomenon more pronounced.

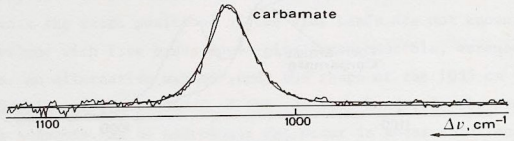


*Fig.8. The Raman spectrum of ammonium carbamate in formamide, after subtraction of the formamide band.*

Apparently, in both cases one band is not entirely sufficient to fit the measured carbamate band completely. Hence, Figs.4 and 8 give another indication for the inherent asymmetry of the carbamate band on the low frequency side, in aqueous as well as non-aqueous solutions. However, Figs. 4 and 8 give no indication of a side-band on the high frequency side of the carbamate band.



4.4. The digital subtraction method applied to spectra of aqueous carbamate solutions

With the new evidence for an intrinsic asymmetry of the carbamate band, the bicarbonate/carbonate concentration ratio was recalculated. Analogous to the procedure applied to the carbamate/formamide spectra, the digital subtraction method was applied to the carbamate/water spectra. For this purpose an aqueous solution of ammonium carbamate with pH > 14 is prepared, to which calcium chloride is added with the intention to precipitate the carbonate present in the solution. Hence, the Raman spectrum of a carbamate solution, free from bicarbonate and carbonate, can be recorded and stored in the computer memory. The spectrum obtained this way is subtracted from spectra recorded at other pH values.

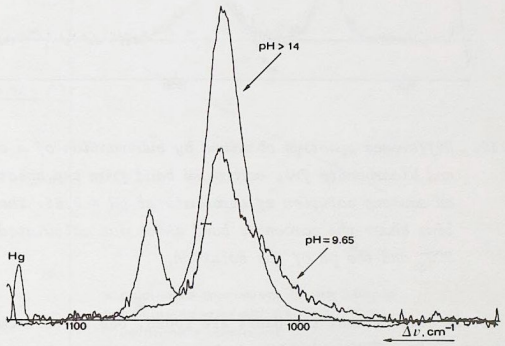


*Fig.9. The Raman spectrum of an aqueous solution of ammonium carbamate of pH = 9.65, together with the spectrum of an aqueous solution of carbamate at pH > 14, to which $CaCl_2$ was added.*

Fig.9 shows the spectrum of an aqueous solution of ammonium carbamate at pH = 9.65 to which the method was applied, together with the pure carbamate spectrum at pH > 14. The spectrum at pH = 9.65 shows the additional band from carbonate at 1065 $cm^{-1}$, and shows strong asymmetry

at the low wavenumber side of the 1035 $cm^{-1}$ band. From the figure it can be seen that a scaling factor must be calculated before subtraction is possible; the wavenumber range for the calculation of this multiplication factor is also shown in Fig.9. Before this is done, the spectra must again be shifted, because, apparently, the position of the carbamate band depends on the pH of the solution. From the different positions of the Hg-line in Fig.9 it can be seen that a shift of approximately 4.5 $cm^{-1}$ is necessary. The figure shows the spectra in the position that gives the best difference spectrum. The difference spectrum is found in Fig.10.

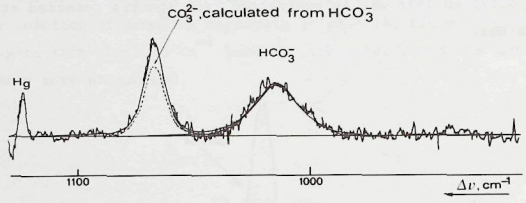


*Fig.10. Difference spectrum obtained by subtraction of a carbonate- and bicarbonate free carbamate band from the spectrum of an aqueous solution of carbamate at pH = 9.65. The dashed line shows the carbonate band which was calculated from $HCO_3^-$ and the pH of the solution.*

It is obvious that two bands are found, one at 1016 $cm^{-1}$, close to the position of the bicarbonate band, and one at the position of the carbonate band. When these bands are completely attributed to bicarbonate and carbonate respectively, the calculated bicarbonate/carbonate ratio is even lower than found when the asymmetry of the carbamate band is not taken into consideration. The carbonate intensity is overestimated and, hence, the corresponding points for the bicarbonate/carbonate concentration ratio, found by this method and shown in Fig.5, differ even more from the results expected theoretically.

If we assume that the band at 1016 $cm^{-1}$ is caused entirely by



$HCO_3^-$, then it is possible to calculate the area expected for the carbonate band from the equilibrium in Eq.(3). The carbonate contribution calculated this way is shown as the dashed line in Fig.10. The difference between the total band area and the contribution of the carbonate band might be attributed to a side-band of carbamate at the high frequency side. If this attribution is correct and if the carbamate band profile is not influenced by the pH of the solution then this calculated difference, divided by the area of the main band of carbamate, should be constant at varying pH.

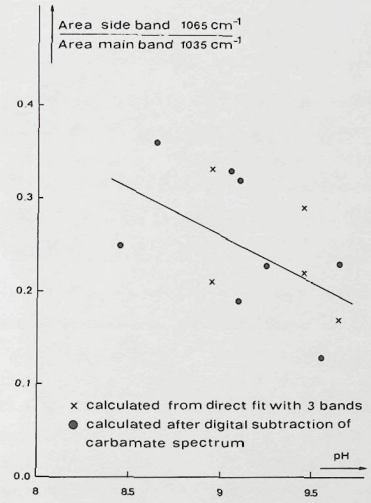


*Fig.11. The area of the high frequency side band, relative to the area of the main band of carbamate vs. the pH.*

Fig.11 shows the result of this procedure. This figure also shows the results of a direct fit with three symmetrical bands. In this case, the subtraction method is not applied, but the carbonate band and, hence, the area of the difference band are calculated directly from

the pH and the area found for the bicarbonate band by the curve-fit routine. It is clear from Fig.11 that both methods yield the same result. The ratio of the high frequency side-band to the main band is obviously influenced by the pH.

From this result we must draw the conclusion that the profile of the carbamate band, at least on the high frequency side, is influenced by the pH. Whether or not the same effect is found on the low frequency side, cannot be told. As we can never be sure, however, that a band found at 1018 $cm^{-1}$ for the carbamate solution, can be attributed entirely to bicarbonate, Raman spectroscopy cannot be used to determine the bicarbonate concentration in solutions that also contain carbamate.

## 5. Discussion

The original goal of the study described in this chapter was to determine whether or not bicarbonate ions are present in aqueous solutions of ammonia and carbon dioxide in order to enable predictions about its presence in urea synthesis mixtures at process conditions.

Indeed, in the Raman spectra of $NH_3/CO_2/H_2O$ mixtures two bands are observed close to the positions of carbamate and bicarbonate. It was found, however, that a straightforward calculation of the bicarbonate concentration from the area of a band found at 1025 $cm^{-1}$, which is close to the position of the bicarbonate band at ambient conditions (1018 $cm^{-1}$), is not possible. The value of 0.3, which was found this way for the bicarbonate/carbamate concentration ratio, is much higher than expected for conditions of $NH_3/CO_2$ = 4.9, $H_2O/CO_2$ = 8.5, p = 3.0 MPa and $61^{\circ}$ C < t < $95^{\circ}$ C. Most likely, this problem is caused by the shape of the carbamate band positioned at 1035 $cm^{-1}$.

While the band found at 1038 $cm^{-1}$ in the Raman spectrum of solid ammonium carbamate is completely symmetrical, the corresponding band found in the polar, non-aqueous solvent formamide, shows a slight asymmetry on the low frequency side. A similar, but more pronounced, asymmetry is found in the spectrum of an aqueous solution of ammonium carbamate at pH > 14. This asymmetry cannot be caused by the presence of $HCO_3^-$, as the concentration ratio bicarbonate/carbonate is approximately 1/4000 at pH = 14. Hence, the asymmetry found in spectra of aqueous, as well as, non-aqueous solutions in an inherent property



of the carbamate species and is probably caused by a side-band at the low frequency side.

A further indication for the asymmetry of the carbamate band was derived from measurements on the $HCO_3^-/CO_3^{2-}$ concentration ratio as a function of the pH, in aqueous solutions of ammonium carbamate, and in aqueous solutions of potassium carbonate. While the results of the measurements in the carbamate free solutions agree well with theory, the results in the presence of carbamate strongly deviate from the expected values. Whereas the presence of a side-band at the low-frequency side of the carbamate band would result in too high values for the $HCO_3^-/CO_3^{2-}$ concentration ratio, in fact, too low values are found at pH < 10. Therefore, the conclusion was drawn that in addition to a side-band at the low frequency side, a side-band must also be present at the high frequency side, close to the position of the carbonate band (1065 $cm^{-1}$).

In two ways the area of this second side-band was calculated from the area of the bicarbonate band and the pH of the solution. Both methods yielded the same result and showed that the area of the side-band at the high frequency side, relative to the area of the main band of carbamate, is influenced by the pH. Hence, it was concluded that the profile of the carbamate band depends on the pH of the solution.

A possible explanation for the asymmetry of the carbamate band is the carbamate ion itself, because it can manifest itself in three different modifications, as can been seen from the following equilibria:

$$H_3N^+-COOH \overset{k_1}{\rightleftarrows} H_3N^+-COO^- \overset{k_2}{\rightleftarrows} H_2N-COO^- \qquad (7)$$

Although the pK values of these equilibria are not known, they can be estimated from the corresponding values[10] of amino acids, listed in Table 5. Probable values are $2 < pK_1 < 3$ and $9 < pK_2 < 10$.

It is unlikely that the $H_3N^+-COOH$ ion can be observed in aqueous solutions of carbamate, because, at the necessary low pH, carbamate decomposes completely into bicarbonate, which, in turn, will decompose into free carbon dioxide that leaves the solution. The presence of the Zwitterion $H_3N^+-COO^-$, however, is quite possible and might account for the increase of the high frequency side-band, near 1065 $cm^{-1}$, with decreasing pH.

| Name | Structure | $pK_1$ | $pK_2$ |
|---|---|---|---|
| Glycine | $H_2N-CH_2-COOH$ | 2.3 | 9.6 |
| Alanine | $H_2N-CH(CH_3)-COOH$ | 2.4 | 9.7 |
| Valine | $H_2N-CH(CH(CH_3)_2)-COOH$ | 2.3 | 9.6 |
| Leucine | $H_2N-CH(CH_2CH(CH_3)_2)-COOH$ | 2.4 | 9.6 |

*Table 5. The pK values of some aliphatic amino acids.*

The presence of the low frequency side-band, at approximately 1025 $cm^{-1}$, cannot be explained this way. Its absence in the solid state spectrum of ammonium carbamate, and its presence in spectra of carbamate solutions at pH > 14, indicate that relatively free moving carbamate ions are required to observe this phenomenon. Hence, most likely the asymmetry on the low frequency side is caused by an asymmetric distribution of the rotational levels.

The conclusions presented above explain the difference between the solid state spectrum and the spectra of solutions of ammonium carbamate. They also account for the fact that the shape of the carbamate band is pH dependent, and, most probably, also pressure and temperature dependent. Therefore, if these conclusions are correct, it is not possible to determine the area of a bicarbonate band in the Raman spectrum of a mixture of carbamate and bicarbonate by subtraction of a carbamate band with a fixed shape, nor is it possible to correct the shape of the carbamate band, because the exact, quantitative p, T and pH dependence is not known.

Hence, the original aim of this part of the study i.e. predicting the bicarbonate concentration in urea synthesis mixtures at process conditions from the bicarbonate concentration in aqueous solutions of ammonia and carbon dioxide at such conditions of p and T that no urea is formed, has not been achieved.



REFERENCES


1. Gorlovskii, D.M. and Kucheryavyi, V.I.
   Zhurn. Prikl. Khim., 1980, 53, 2348
2. Newman, S.A.
   "Thermodynamics of Aqueous Systems with Industrial Applications",
   A.C.S. Symp. Series, 1980, 133, 139
3. Kotula, E.
   J. Chem. Techn. Biotechnol., 1981, 31, 103
4. "Handbook of Chemistry and Physics",
   C.R.C. press, Ed. R.C. Weast, 54th ed., 1973-1974
5. Cunningham, K.M., Goldberg, M.C. and Weiner, E.R.
   Anal. Chem., 1977, 49, 70
6. Herzberg, G.
   "Infrared and Raman Spectra", Van Nostrand,
   New York, 1945
7. Frasco, D.L.
   J. Chem. Phys., 1964, 41, 2134
8. Hisatsune, I.C.
   Can. J. Chem., 1984, 62, 945
9. Davis, A.R. and Oliver, B.G.
   J. Solution Chem., 1972, 1, 329
10. Mahler, H.R. and Cordes, E.H.
    "Biological Chemistry", 2th ed., Harper and Row, New York, 1971

SUMMARY

This thesis describes the benefits and shortcomings of Laser Raman Spectrometry for the quantitative analysis of urea synthesis mixtures at process conditions.

In the first chapter the principle of the Raman effect is explained and the important influence of the invention of the laser on the application of the linear, as well as, the non-linear Raman effects is shown.

The review presented in chapter two shows, in general, the possibilities of laser Raman spectrometry for quantitative analysis. In this chapter we also discuss some factors which influence the intensity of a Raman band, like intensity, frequency and polarization of the incident radiation and sample characteristics, like colour and index of refraction. The use of the computer programs, which are described in this chapter as well, is necessary because of the strong band overlap that occurs in the Raman spectra of urea synthesis mixtures.

Chapter three shows that all components of the urea synthesis give a characteristic Raman band, and reveals that the detection limits of urea and ammonium carbamate are sufficiently low for the determination of the concentrations at process conditions. In this chapter we also show that, except for ammonia, no effect of pressure on the relative intensities of the components is expected. On the contrary, all bands in the spectrum of the mixture will be affected by temperature. This effect will be reduced partially by the use of an internal standard, but corrections have to be made with, for example, the population factors. The chapters two and three show that quantitative Raman spectrometry benefits from the use of an internal standard.

In chapter four we present the results from measurements on the conversion of carbon dioxide to urea. The results found are in good agreement with results found in literature, which were obtained with another analytical method. It must be stated, however, that the method is generally applicable only if the bicarbonate concentration in the mixture is negligible, since our curve-fit program cannot fit Raman spectra of mixtures that contain urea and bicarbonate simultaneously. This is due to the fact that the line separation between urea (1005 $cm^{-1}$) and bicarbonate (1018 $cm^{-1}$) is too small to be distinguished by the program.

The measurements on aqueous solutions of ammonia and carbon dioxide,

presented in chapter five, were performed to examine whether or not the presence of bicarbonate should be expected in urea synthesis mixtures at process conditions. This aim was not achieved, because it was not possible to obtain unambiguous results for the area of the bicarbonate band from the Raman spectra of mixtures containing both carbamate and bicarbonate. This is caused by the fact that the bicarbonate band is situated on the flank of the carbamate band. The shape of the latter, however, is probably pH dependent.



SAMENVATTING

Toen in 1928 door C.V. Raman en K.S. Krishnan voor het eerst het Raman effekt werd waargenomen stond ook de infrarood spektrometrie nog in haar kinderschoenen. Metingen in het verre infrarood en in het microgolf bereik waren niet mogelijk, en metingen die tegenwoordig routinematig uitgevoerd worden waren moeilijk en tijdrovend. Het is daarom niet verwonderlijk dat deze nieuwe vorm van molekuul spektrometrie met grote belangstelling werd ontvangen. Het belangrijkste voordeel van Raman spektrometrie ten opzichte van infrarood spektrometrie was toen, en is nog steeds, het feit dat de rotatie- en vibratieovergangen in molekulen kunnen worden waargenomen in het zichtbare gedeelte van het spektrum.

Door de ontwikkeling van snellere en betere infrarood absorptie technieken na de tweede wereldoorlog en door de opkomst van de microgolf spektrometrie in de jaren vijftig, kwam de Raman spektrometrie echter op het tweede plan te staan. Een belangrijk probleem in de Raman spektrometrie is altijd de relatief lage intensiteit van het Raman effekt geweest. Het ontbreken van intensieve, monochromatische lichtbronnen heeft daarom mede bijgedragen tot deze terugval in belangstelling.

De hernieuwde interesse in de Raman spektrometrie in de afgelopen decennia is dan ook een logisch gevolg van de ontdekking van de laser in het begin van de zestiger jaren. De laser een zeer krachtige, gerichte lichtbron maakte het mogelijk metingen uit te voeren aan kleine monsters ($10^{-6}$ ml voor vloeistoffen) en zorgde voor een duidelijke verlaging van de detektiegrenzen en voor een drastische verkorting van de meetduur.

Van het begin af was de kwalitatieve analyse de sterkste kant van de Raman spektrometrie. De methode blijkt, naast infrarood spektrometrie, uitermate geschikt voor struktuurbepaling en voor het aantonen van funktionele groepen in molekulen. De kwantitatieve toepassing is minder ontwikkeld, wat vooral te wijten is aan de zwakte van het effekt. Het in dit proefschrift beschreven onderzoek toont aan dat de Raman spektrometrie als kwantitatieve analysemethode zeker bruikbaar is, zelfs onder tamelijk extreme omstandigheden.

Als voorbeeld werd de ureum synthese gekozen. Ureum wordt bereid via een twee-traps reaktie volgens

$$2NH_3 + CO_2 \rightleftarrows H_2NCOONH_4$$

$$H_2NCOONH_4 \rightleftarrows H_2NCONH_2 + H_2O$$

De normale proceskondities zijn een temperatuurgebied van 170-210 °C en een drukbereik van 15-25 MPa. Daar een temperatuur- of drukverandering een aanzienlijke verandering van de samenstelling van het reaktiemengsel zal geven, moet voor de analyse van de samenstelling de voorkeur worden gegeven aan een in-situ methode. Hiervoor is een spektrometrische methode bij uitstek geschikt.

In dit geval kunnen de gangbare methoden echter niet gebruikt worden. Met behulp van UV-spektrometrie zou men wel informatie verkrijgen met betrekking tot de carbonylverbindingen en ammonia, maar niet voor water. Het infrarood spektrum van het mengsel daarentegen zal grotendeels onbruikbaar zijn door de aanwezigheid van een zeer brede water band. Laser Raman spektrometrie lijkt daarom de meest aangewezen analysemethode. Water is een geschikt oplosmiddel en alle bij de reaktie betrokken komponenten, inklusief water bezitten een karakteristieke Raman band.

In het eerste hoofdstuk van dit proefschrift wordt het principe van het Raman effekt uitgelegd en wordt gewezen op het belang van de uitvinding van de laser voor de ontwikkeling van de lineaire Raman spektrometrie en voor de praktische toepassing van de niet-lineaire Raman effekten.

In hoofdstuk twee vindt men, in een literatuuroverzicht, de belangrijkste toepassingsgebieden van de kwantitatieve Raman spektrometrie. Ook worden hier enkele faktoren behandeld die de intensiteit van een Raman band kunnen beinvloeden, zoals intensiteit, golflengte en polarisatie eigenschappen van het invallende licht en monstereigenschappen, zoals brekingsindex en kleur. In dit hoofdstuk worden tevens de komputerprogramma's beschreven die gebruikt werden bij de verwerking van de Raman spektra. Het gebruik van een curve-fit programma is noodzakelijk door de sterke bandoverlap die optreedt in de spektra van ureum synthese mengsels.

In het derde hoofdstuk wordt aangetoond dat elk van de bij de ureum synthese betrokken komponenten een karakteristieke Raman band bezit, bijvoorbeeld ureum op 1005 $cm^{-1}$ en ammonium carbamaat op 1035 $cm^{-1}$. De detektiegrenzen van ureum en carbamaat blijken laag genoeg te zijn om de betreffende concentraties onder proceskondities te kunnen meten. Aan modelstoffen werd de invloed van druk en temperatuur op de intensiteit van Raman banden onderzocht. Voor geen der gebruikte stoffen werd een significante verandering van het Raman spektrum ten gevolge van drukveranderingen gevonden. Wel bleek dat de intensiteit van Raman banden verandert met de temperatuur. Voor deze temperatuurseffekten kan echter worden gecorrigeerd, enerzijds door gebruik te maken van een interne standaard (thermische expansie), anderzijds door berekening van de noodzakelijke correctie faktoren (bezettingsgraad van de energieniveaus). In de hoofdstukken twee en drie wordt aangetoond dat de interne standaard een onmisbaar hulpmiddel is in de kwantitatieve Raman spektrometrie.

In hoofdstuk vier worden de resultaten gepresenteerd van metingen aan de omzetting van kooldioxide naar ureum. De metingen werden uitgevoerd onder proceskondities en de waarden die werden gevonden voor de conversie van $CO_2$ naar ureum stemmen zeer goed overeen met in de literatuur gemelde waarnemingen die gevonden werden met een andere analysemethode. Raman spektrometrie blijkt dus een geschikte methode te zijn voor de kwantitatieve analyse van ureum synthese mengsels, mits aan enige voorwaarden wordt voldaan. De belangrijkste eis is dat de mengsels geen bicarbonaat bevatten. De bicarbonaat band is namelijk gelegen op 1018 $cm^{-1}$, dus tussen de banden van ureum en ammonium carbamaat. Met het door ons gebruikte curve-fit programma zijn we echter (nog) niet in staat de afzonderlijke bijdrage van elk van deze banden in het Raman spektrum van een mengsel van deze stoffen te bepalen.

De metingen aan waterige oplossingen van ammoniak en kooldioxide, beschreven in hoofdstuk vijf, werden uitgevoerd om na te gaan of de aanwezigheid van bicarbonaat onder ureum synthese kondities te verwachten is. Tijdens het onderzoek bleek dat geen ondubbelzinnige resultaten voor de intensiteit van de bicarbonaat band verkregen konden worden. Dit probleem blijkt veroorzaakt te worden door de vorm van de ammonium carbamaat band. De vorm van deze band blijkt afhankelijk te zijn van de pH, waardoor de intensiteit van de bicarbonaat band, die op een flank van deze band gelegen is, niet juist kan worden bepaald.

ACKNOWLEDGEMENT

A grant from the Dutch State Mines (DSM) Geleen to the author of this thesis is gratefully acknowledged.

Receptie na afloop van de promotie
in de aula van de
Technische Hogeschool Delft

MARTIN VAN ECK EN TRUJA EEKHOUT

Delft

STELLINGEN

1. De gekonstateerde voordelen van het gebruik van korte chemisch gebonden ketens als stationaire fase voor de reversed phase chromatografie van eiwitten, zijn een logisch gevolg van het feit dat voor grote molekulen de retentie sterk varieert met de kompositie.

2. De theoretische beschouwingen van Peaden en Lee over superkritische chromatografie worden sterk vertekend door de onjuiste aanname van een lineair verband tussen dichtheid en druk.

   Peaden, P.A. and Lee, M.L., J.Chromatogr., 1983, 259, 1.

3. De hoge intensiteit van de OH-banden bij het low-flow ICP van Rezaaiyaan en Hieftje is niet te wijten aan een inherente eigenschap van dit plasma, zoals wordt gesuggereerd, maar wordt veroorzaakt door een te hoog monster-introduktiedebiet.

   Rezaaiyaan, R. and Hieftje, G.M., Anal.Chem., 1985, 57, 412.

4. De klassifikatie van parallelle processoren naar hun programmeerniveaus, zoals voorgesteld door Flynn en later in een gemodificeerde vorm door Zimmermann en Sips, is veel te rudimentair om van praktische betekenis te kunnen zijn.

   Flynn, M.J., "Some computer organizations and their effectiveness", IEEE Transactions on Computers, 1972, C-21.

   Zimmermann, N.J. and Sips, H.J., "Parallel data verwerken", Informatie, 1978, 20.

5. De toepassing van Raman spektrometrie voor de geautomatiseerde, kwantitatieve analyse van fenolmengsels in water zal grote problemen met zich meebrengen, indien andere fenolen aanwezig zijn.

   Marley, N.A., Mann, C.K. and Vickers, T.J., Appl.Spectrosc., 1984, 38, 540.

6. De neiging om bij de optimalisering van vloeistofchromatografische scheidingen te veel te automatiseren heeft bij de huidige stand van zaken nadelige gevolgen voor het bereiken van het beste resultaat.

7. De resultaten van de in de microbiologie algemeen toegepaste methode voor de bepaling van zwavelverbindingen volgens Pachmayer, moeten sterk te denken geven, daar men nauwelijks rekening houdt met de belangrijke onderlinge interferenties die op kunnen treden.

   Pachmayer, "Vorkommen und Bestimmung von Schwefelverbindungen in Mineralwasser", Thesis, München, 1960.

8. Het voorschrijven van de potentie D30 van het homeopatisch geneesmiddel "Aconitum" bij de behandeling van rugklachten voorkomt weliswaar acute vergiftigingsverschijnselen bij de patient, maar de vraag lijkt gerechtvaardigd of het middel in een dergelijke verdunning ($1:10^{30}$) nog wel werkzaam is.

9. Het begrip "reageerbuisbaby" krijgt pas werkelijk inhoud als chemici in staat blijken een levend organisme te creëren uit een oermassa van koolstof, zuurstof, stikstof en waterstof.